Floquet Topological Superconductors

Master's Thesis in Applied Mathematics

Jimmy Aronsson

May 25, 2018

Contents

Introduction

Summary

Over the past decade, much work has gone into classifying topological insulators and topological superconductors. These are exotic types of crystalline materials characterized by their ability to support robust surface states, which allow the formation of an electric or spin current along the surface of the crystal. Interestingly, the surface states are topologically protected from destructive interference and the surface current is therefore extremely robust. Experimental dfficulties have led researchers to look at periodic driving as a way of inducing topologically nontrivial behaviour in otherwise trivial systems. Such *Floquet topological insulators* and *superconductors* have been experimentally observed and are currently being classified. In this thesis, we perform a homotopy classification of particle-hole symmetric Floquet topological insulators and as an important by-product, we achieve a classification of Floquet topological superconductors.

History

The history of topological quantum matter starts in 1980 with von Klitzing's experimental discovery of the quantum Hall effect [19]. Subjecting an ultracold two-dimensional crystalline material to a perpendicular magnetic field may cause an electric current to form along the crystal boundary, and as the magnetic field strength is increased, the Hall conductance becomes quantized:

$$\sigma_H = \frac{e^2}{h}\nu, \qquad \nu = 0, 1, 2, 3, \ldots,$$

where e is the elementary charge and h is Planck's constant. Remarkably, the quantized Hall conductance was found to be "insensitive to the geometry of the device", displaying a robustness that had never before been observed. The theoretical explanation came two years later, in 1982, when Thouless, Kohomoto, Nightingale, and de Nijs were able to derive the quantized Hall conductance and proved the integer factor ν to be a topological invariant [34]. For his discovery, von Klitzing was awarded the 1985 Nobel prize.

It was Haldane who discovered [13] that topological phenomena can arise even without a macroscopic magnetic field. Instead, Haldane's graphene model for the quantum Hall effect relies on *time reversal symmetry breaking*. Switching on a magnetic field is one way to break time reversal symmetry but it is not the only way, so Haldane's model put the quantum Hall effect in a more general setting. The next major breakthrough came 17 years later, in 2005, when Kane and Mele proposed a graphene model of the quantum *spin* Hall effect [15]; spin is an intrinsic form of angular momentum that in the case of electrons take on two values called *spin up* and *spin down*. Kane and Mele's model can be described as two copies of Haldane's model for the ordinary quantum

Hall effect, one in which spin up-electrons propagate in one direction and one in which spin down-electrons propagate in the opposite direction. Each copy induces an electric current around the crystal boundary and though the net charge current vanishes, a net *spin* current survives. The model is characterized by a $\mathbb{Z}_2$ topological invariant and does not break time reversal symmetry. Today, topological quantum matter is a major research area within condensed matter physics and Thouless, Haldane, and Kosterlitz were awarded the 2016 Nobel prize for their contributions.

The search for topological materials has revealed hundreds of potential candidates, some of which have been experimentally verified, but this is just a small proportion of the total number of known crystalline structures [6]. To make things worse, many of the known candidate materials are difficult to engineer. In an attempt to solve this problem, researchers are examining the possibilities of inducing topological behaviour in otherwise trivial systems by means of a periodic driving interaction, as the dynamical evolution of a quantum system is relatively easy to control. Not only have such *Floquet* topological materials been observed in a number of settings [22, 23, 35], their topological features are in a sense richer than that of their static counterparts [26].

Outline

Chapter 1 provides the reader with an introduction to quantum mechanics, primarily aimed at mathematicians and with particular focus on the time-evolution operator that encapsulates the dynamical evolution of a time-dependent quantum system. Chapter 2 deals with crystal lattices, band theory, topological insulators and topological invariants, Chern numbers being an important example. In Chapter 3, we discuss periodically driven (Floquet) systems and quasienergy bands, before introducing the concept of particle-hole symmetry and describing its relation to superconductivity. The remainder of this final chapter is then devoted to the classification of Floquet topological insulators with particle-hole symmetry. We use a general classification scheme originally developed by Rudner [26] and which has later been applied to time-reversal invariant systems [8].

Acknowledgements

This project has taken me on a fascinating journey through the realm of theoretical physics that would not have been possible without the support of my advisor Prof. Henrik Johannesson, to whom I want to express my sincere gratitude. His enthusiasm, encouragement, and expertise has had a tremendous impact on my success. I would also like to thank my examiner Prof. Hjalmar Rosengren and opponent Johan Davegård for their insightful comments.

My sincere thanks goes to Bogdan Dobondi, Zakarias Sjöström Dyrefelt, Jens Roderus, and the rest of my friends at the mathematics and physics departments, with whom I have had many interesting discussions. Their suggestions have aided me at every stage of the process.

Finally, I want to thank my family for their endless and unconditional support.

1

Quantum Mechanics

"One of the faults of mathematicians is: when physicists give them an equation, they take it absolutely seriously."

– Henry McKean

A hallmark of 20^{th} century physics, quantum mechanics is perhaps the most successful scientific theory in history, having correctly predicted and explained a plethora of phenomena and experimental results with unprecedented accuracy. Its abstract mathematical framework and often unintuitive interpretations, on the other hand, makes quantum mechanics a difficult subject to learn. In this introductory chapter, we have chosen a rather formal and concise approach aimed mainly at mathematicians, although physics students should have no problem following the discourse. Relevant parts of the mathematical framework are formally introduced, their properties rigorously proven and their connections to physics presented as a series of postulates. It is difficult to build a solid foundation in just a few pages, however, so interested readers are strongly encouraged to read the more comprehensive introductions given in the standard literature [12, 27, 31].

The chapter ends with a detailed analysis of the *time-evolution operator* used to evolve quantum systems in time. We prove results on convergence, unitarity, and other important properties which are conventionally left unproven in the physics literature.

1.1 Basic notions

When studying physical phenomena such as electrical conduction in crystals, any attempt to include all relevant parameters and interactions from the get-go is sure to fail, the system would simply be too complex. Physicists therefore restrict their attention to a few "relevant" parameters and interactions while putting aside those which do not significantly contribute to the overall dynamics, including most environmental effects or lattice vibrations at low temperatures. When a simple system is well understood, previously ignored parameters can be reintroduced, expanding the theory to more realistic scenarios and improving correspondence with experimental results. A (dynamical) quantum system can therefore be viewed as a universe of its own, subject only to those interactions and environmental effects that one has chosen to include or that arise naturally, and the mathematical object used to model such systems is a complex Hilbert space.

Postulate 1. *Any quantum system is described by a corresponding complex Hilbert space $\mathcal{H}$. Quantum states are represented by elements of $\mathcal{H}$.*

This postulate is rather vague as the contextual meaning of the words *described* and *represented* has not been adequately explained. One reason, in addition to the author's inexperience, is that no one quite knows how quantum mechanics should be interpreted; we can work out mathematical details and correctly predict the outcomes of experiments but the true workings of nature are ultimately unknown. Nevertheless, it is possible to justify the use of complex Hilbert spaces in physics, see for example J.J. Sakurai's exposition of the Stern-Gerlach experiment [27].

Our analysis of topological insulators will be conducted for finite-dimensional Hilbert spaces, but most of the material presented in this introductory chapter is equally valid in the more general separable case and will therefore be presented without explicit mention to the dimensionality.

Definition (bra, ket)**.** Let $\mathcal{H}$ be a complex Hilbert space with dual space $\mathcal{H}^*$.

1. A *ket vector*, or *ket*, is an element $|\psi\rangle \in \mathcal{H}$,
2. A *bra vector*, or *bra*, is an element $\langle\psi| \in \mathcal{H}^*$.

Kets are used to represent quantum states and the two terms are often used interchangably, but the relationship is not precisely one-to-one. We will discuss this in more detail later on but the short story is that multiplication by scalar, $|\psi\rangle \mapsto \lambda\,|\psi\rangle$, does not change the underlying state.

By duality, any bra vector $\langle\psi|$ can be treated as the conjugate transpose of a ket vector $|\psi\rangle$ and vice versa, and the inner product on $\mathcal{H}$ is denoted by juxtaposition of bras with kets[1]

$$|\phi_1\rangle \in \mathcal{H}, \quad |\phi_2\rangle \in \mathcal{H} \qquad \mapsto \qquad \langle\phi_1|\phi_2\rangle \in \mathbb{C}.$$

Bras and kets can also be multiplied to form operators[2]

$$\langle\phi_1| \in \mathcal{H}^*, \quad |\phi_2\rangle \in \mathcal{H} \qquad \mapsto \qquad |\phi_2\rangle\,\langle\phi_1| \in \mathrm{Hom}(\mathcal{H}).$$

The beauty of Dirac notation is its associativity: the expression

$$|\phi_1\rangle\,\langle\phi_2|\phi_3\rangle$$

can be interpreted both as the operator $|\phi_1\rangle\,\langle\phi_2|$ acting on the ket $|\phi_3\rangle$, and as the ket $|\phi_1\rangle$ multiplied by the scalar $\langle\phi_2|\phi_3\rangle$, and both of these interpretations yield the same element of $\mathcal{H}$. Expressions involving several bras and kets can therefore be interpreted in many different ways - a very powerful fact, as illustrated by the following example.

Example 1. Let $\{|\psi_n\rangle\}$ be an orthonormal basis for $\mathcal{H}$ and note that the identity operator on $\mathcal{H}$ takes the matrix form

$$\mathbb{1} = \sum_n |\psi_n\rangle\,\langle\psi_n|\,.$$

Any ket $|\phi\rangle \in \mathcal{H}$ can be written as a linear combination

$$|\phi\rangle = \mathbb{1}\,|\phi\rangle = \sum_n |\psi_n\rangle\,\langle\psi_n|\phi\rangle = \sum_n c_n\,|\psi_n\rangle\,,$$

[1] Dirac notation is completely analogous to writing $\mathbf{u}$ for (column) vectors and $\mathbf{u}^\dagger$ for dual (row) vectors, where the dagger † is used to denote conjugate transpose. The inner product $\langle\phi_1|\phi_2\rangle$ is therefore analogous to the expression

$$\mathbf{u}\cdot\mathbf{v} = \mathbf{u}^\dagger\mathbf{v}$$

for the inner product between vectors $\mathbf{u}, \mathbf{v}$.

[2] This is analogous to column vectors $\mathbf{u}$ and row vectors $\mathbf{v}^\dagger$ being multiplied to form matrices $\mathbf{u}\mathbf{v}^\dagger$.

where $c_n = \langle \psi_n | \phi \rangle$ is the n'th coordinate, and the inner product on $\mathcal{H}$ can be evaluated as[3]

$$\langle \phi | \chi \rangle = \langle \phi | \mathbb{1} | \chi \rangle = \langle \phi | \left(\sum_n |\psi_n\rangle \langle \psi_n| \right) |\chi\rangle = \sum_n \langle \phi | \psi_n \rangle \langle \psi_n | \chi \rangle = \sum_n \langle \psi_n | \phi \rangle^* \langle \psi_n | \chi \rangle .$$

It should be noted that associativity fails to hold in certain situations. Consider, for example, the expression $\langle \psi | A | \phi \rangle$ where A is an arbitrary operator on $\mathcal{H}$. This expression can be interpreted as the scalar product between $|\psi\rangle$ and $A|\phi\rangle$, or as the scalar product between $A^\dagger |\psi\rangle$ and $|\phi\rangle$, but the latter interpretation presupposes the existence of the Hermitian adjoint $A^\dagger$. As associativity is commonly used to cleverly rewrite expressions both when proving new results and when performing calculations, Dirac notation can be tricky to use when studying unbounded operators on infinite-dimensional spaces or other operators for which the existence of adjoints is not guaranteed, but rest assured: every operator relevant to our purposes does have a Hermitian adjoint. In fact, most of the interesting operators used in quantum mechanics are self-adjoint (*Hermitian*):

$$A = A^\dagger$$

Hermitian operators are key objects for translating mathematical results back into physical terms. The most important operator in quantum mechanics is the *Hamiltonian*, a Hermitian operator that describes the energy structure of the system in question and that completely determines the dynamical evolution of the quantum states, as we shall see in the next section.

Example 2. Consider a quantum system $\mathcal{H}$ describing an electron in orbit about a nucleus. The electron energy depends on the distance r between the electron and the nucleus but, as anyone familiar with the term *electron shell* will recall, only a discrete set of distances r are allowed, hence only a discrete set of *energies* are allowed. These energies turn out to be the eigenvalues of the Hamiltonian operator

$$H = \frac{p^2}{2m_e} + V(r),$$

where p is the momentum operator, m_e is the electron mass, and $V(r)$ is the Coulomb potential. The energy spectrum thus coincides with the functional analytical spectrum of the Hamiltonian.

This connection between observables and eigenvalues of Hermitian operators is general.

Postulate 2. *Every observable property is represented by a Hermitian operator, the eigenvalues of which determine the possible observable values.*

We use the word *observable* to denote both the observable property per se - such as position, momentum, or energy - and the Hermitian operator that represents it. The correspondence between observables and Hermitian operators is not one-to-one, however, as there are Hermitian operators which are not observables. The strive towards understanding observables has resulted in a number of important functional analytical notions such as C^*-algebras, illustrating one of the many ways in which the histories of quantum mechanics and functional analysis are intertwined.

Our next result is useful when studying observables in finite-dimensional systems.

[3]This is the Dirac analogue of the relation more commonly expressed as

$$\mathbf{u} \cdot \mathbf{v} = \sum_n u_n v_n^*,$$

the difference being that Dirac's inner product is antilinear in the first argument rather than in the second.

Proposition 1. *Denote by $M_N(\mathbb{C})$ the set of complex $N \times N$-matrices. The subset*

$$H_N(\mathbb{C}) = \left\{ A \in M_N(\mathbb{C}) : A = A^\dagger \right\}$$

of Hermitian $N \times N$-matrices forms a vector space over $\mathbb{R}$. Furthermore, $\dim_{\mathbb{R}} H_N(\mathbb{C}) = N^2$.

Proof. The set $M_N(\mathbb{C})$ is known to be a complex vector space and is therefore also a real vector space, so it suffices to prove that the subset $H_N(\mathbb{C})$ is closed under addition and multiplication by real scalar. Indeed, for all $\alpha_1, \alpha_2 \in \mathbb{R}$ and all $H_1, H_2 \in H_N(\mathbb{C})$,

$$(\alpha_1 H_1 + \alpha_2 H_2)^\dagger = \alpha_1^* H_1^\dagger + \alpha_2^* H_2^\dagger = \alpha_1 H_1 + \alpha_2 H_2. \tag{1.1}$$

The dimension can easily be computed in the case $N = 2$ by noting that any Hermitian 2×2-matrix has to be on the form

$$H = \begin{pmatrix} \alpha & \gamma + i\delta \\ \gamma - i\delta & \beta \end{pmatrix} = \alpha \begin{pmatrix} 1 & 0 \\ 0 & 0 \end{pmatrix} + \beta \begin{pmatrix} 0 & 0 \\ 0 & 1 \end{pmatrix} + \gamma \begin{pmatrix} 0 & 1 \\ 1 & 0 \end{pmatrix} + \delta \begin{pmatrix} 0 & i \\ -i & 0 \end{pmatrix}$$

where $\alpha, \beta, \gamma, \delta \in \mathbb{R}$. In other words, the four Hermitian matrices on the right-hand side span $H_2(\mathbb{C})$ and as they are clearly linearly independent, they constitute a basis. The corresponding basis in the case $N = 3$ is

$$\text{Diagonal entries:} \quad \begin{pmatrix} 1 & 0 & 0 \\ 0 & 0 & 0 \\ 0 & 0 & 0 \end{pmatrix}, \quad \begin{pmatrix} 0 & 0 & 0 \\ 0 & 1 & 0 \\ 0 & 0 & 0 \end{pmatrix}, \quad \begin{pmatrix} 0 & 0 & 0 \\ 0 & 0 & 0 \\ 0 & 0 & 1 \end{pmatrix},$$

$$\text{Off-diagonal, real parts:} \quad \begin{pmatrix} 0 & 1 & 0 \\ 1 & 0 & 0 \\ 0 & 0 & 0 \end{pmatrix}, \quad \begin{pmatrix} 0 & 0 & 1 \\ 0 & 0 & 0 \\ 1 & 0 & 0 \end{pmatrix}, \quad \begin{pmatrix} 0 & 0 & 0 \\ 0 & 0 & 1 \\ 0 & 1 & 0 \end{pmatrix},$$

$$\text{Off-diagonal, imaginary parts:} \quad \begin{pmatrix} 0 & i & 0 \\ -i & 0 & 0 \\ 0 & 0 & 0 \end{pmatrix}, \quad \begin{pmatrix} 0 & 0 & i \\ 0 & 0 & 0 \\ -i & 0 & 0 \end{pmatrix}, \quad \begin{pmatrix} 0 & 0 & 0 \\ 0 & 0 & i \\ 0 & -i & 0 \end{pmatrix},$$

and we can easily extend this pattern to arbitrary N. As we need N different matrices to represent the diagonal entries and $\frac{N^2-N}{2}$ different matrices both for the real parts and the imaginary parts of the $N^2 - N$ off-diagonal entries, the dimension is

$$\dim_{\mathbb{R}} H_N(\mathbb{C}) = N + \frac{N^2 - N}{2} + \frac{N^2 - N}{2} = N^2.$$

□

Remark 1. The space $H_N(\mathbb{C})$ is not a *complex* vector space, as the second equality in Eq. (1.1) does not hold for arbitrary complex scalars.

Corollary 1. *The Pauli matrices*

$$\sigma_x = \begin{pmatrix} 0 & 1 \\ 1 & 0 \end{pmatrix}, \quad \sigma_y = \begin{pmatrix} 0 & i \\ -i & 0 \end{pmatrix}, \quad \sigma_z = \begin{pmatrix} 1 & 0 \\ 0 & -1 \end{pmatrix},$$

form a basis for the space of traceless Hermitian 2×2-matrices. Together with the identity matrix

$$\sigma_0 = \begin{pmatrix} 1 & 0 \\ 0 & 1 \end{pmatrix},$$

they form a basis for $H_2(\mathbb{C})$.

The Pauli matrices are important in quantum mechanics for a number of reasons, including:

1. Many problems in quantum mechanics are difficult to solve analytically and quickly become computationally demanding. Progress can then be made by restricting attention to the two lowest energy states, called the *ground state* and the *first excited state*, thereby obtaining a 2-dimensional Hilbert space and a Hamiltonian that can be expressed using Pauli matrices.

2. Multiplying the Pauli matrices by i yields a basis for the real space of traceless anti-Hermitian[4] 2×2-matrices, which constitute the defining representation of the Lie algebra $\mathfrak{su}(2)$. The Pauli matrices can therefore be used to study the observables *angular momentum* and *spin*, both of which are understood in terms of irreducible representations of $SU(2)$.

Next up is the ever important spectral theorem [10].

Spectral Theorem. *Let A be a compact[5] Hermitian operator on a Hilbert space $\mathcal{H}$. Then $\mathcal{H}$ admits an orthonormal basis $\{|a_n\rangle\}$ consisting of eigenstates of A. Moreover, for every $|\psi\rangle \in \mathcal{H}$,*

$$A\,|\psi\rangle = \sum_n a_n\,|a_n\rangle\,\langle a_n|\psi\rangle\,,$$

where a_n is the eigenvalue corresponding to the eigenket $|a_n\rangle$.

The spectral theorem allows us to write any Hermitian operator A on the simple form

$$A = \sum_n a_n\,|a_n\rangle\,\langle a_n|\,, \tag{1.2}$$

although the notation is slightly different in the special case of the Hamiltonian

$$H = \sum_n E_n\,|E_n\rangle\,\langle E_n|\,,$$

as we prefer the letter E to the letter H when working with energies.

Returning to the electron in nuclear orbit, we now know that the eigenvalues E_n of the Hamiltonian H determine the *possible* electron energies, but what determines the *actual* energy? Surely, the electron can only have a definite energy at any given time? This is where it gets interesting, because the answer to the last question is *no*; the electron can be in a superposition

$$|\psi\rangle = \langle E_1|\psi\rangle\,|E_1\rangle + \langle E_2|\psi\rangle\,|E_2\rangle + \cdots$$

of energy states, in which case the energy has no definite value. When the electron is in the state

$$|\psi\rangle = \frac{1}{2}\,|E_1\rangle + \frac{\sqrt{3}i}{2}\,|E_2\rangle\,,$$

for example, any device that measures the electron energy has a 25% probability of returning the value E_1 and a 75% probability of returning the value E_2. One way to interpret this strange finding would be that nature does not "decide" upon a particular energy until the energy is somehow measured, although this interpretation only raises the question of what constitutes a measurement. Attempts to resolve this *measurement problem* have spawned a large number of interpretations of quantum mechanics, perhaps the most popular of which are the *Copenhagen* and *many worlds* interpretations, but the problem ultimately remains unresolved [7, 29].

[4] An operator A is called *anti-Hermitian*, or *skew-Hermitian*, if $A^\dagger = -A$.

[5] Compactness is automatically satisfied in the finite-dimensional case.

In this thesis, we choose the popular *shut up and calculate* approach that most students of quantum mechanics eventually end up taking: as long as our postulates and mathematical results can be used to predict the outcomes of experiments, we do not spend too much time worrying about *why* they can. So let us get back to the action.

Postulate 3. *Performing a measurement of an observable A, in the state represented by $|\psi\rangle$, yields the measured value a_n with probability $P(a_n) = |\langle a_n|\psi\rangle|^2$.*

We will take a somewhat closer look at this postulate in a moment.

Quantum mechanics has been developed in order to understand how nature works at very small scales but it can in principle be applied even at macroscopic scales. It is therefore possible to test quantum mechanical predictions by comparing them with those of classical mechanics. The quantum analogue of a classical dynamical variable $a(t)$ turns out to be the state-dependent expectation value

$$\langle A\rangle = \langle\psi|A|\psi\rangle$$

of the corresponding observable A; the expectation values of position x and momentum p in the quantum harmonic oscillator, for instance, can be proven [37] to satisfy Newton's equations

$$\frac{\mathrm{d}}{\mathrm{d}t}\langle x\rangle = \frac{1}{m}\langle p\rangle, \qquad \text{and} \qquad \frac{\mathrm{d}}{\mathrm{d}t}\langle p\rangle = -m\omega^2\langle x\rangle = -V'(\langle x\rangle).$$

Proposition 2. *The quantum mechanical definition of expectation value, $\langle A\rangle = \langle\psi|A|\psi\rangle$, coincides with the standard definition of the expectation value of a discrete random variable A:*

$$\langle A\rangle = \sum_n a_n P(a_n),$$

where $P(a_n) = |\langle a_n|\psi\rangle|^2$ is the state-dependent probability associated with the outcome a_n.

Proof. By the spectral theorem,

$$\langle\psi|A|\psi\rangle = \langle\psi|\left(\sum_n a_n |a_n\rangle\langle a_n|\right)|\psi\rangle = \sum_n a_n \langle\psi|a_n\rangle\langle a_n|\psi\rangle = \sum_n a_n |\langle a_n|\psi\rangle|^2 = \sum_n a_n P(a_n).$$

□

Example 3. We return once more to the electron in nuclear orbit. Assuming the electron to be in the state

$$|\psi\rangle = \frac{1}{2}|E_1\rangle + \frac{\sqrt{3}i}{2}|E_2\rangle,$$

the energy expectation value can be computed either directly from the definition,

$$\begin{aligned}\langle\psi|H|\psi\rangle &= \left(\frac{1}{2}\langle E_1| - \frac{\sqrt{3}i}{2}\langle E_2|\right) H \left(\frac{1}{2}|E_1\rangle + \frac{\sqrt{3}i}{2}|E_2\rangle\right) = \\ &= \frac{1}{4}\langle E_1|H|E_1\rangle - \frac{\sqrt{3}i}{4}\langle E_1|H|E_2\rangle + \frac{\sqrt{3}i}{4}\langle E_2|H|E_1\rangle + \frac{3}{4}\langle E_2|H|E_2\rangle = \\ &= \frac{1}{4}E_1\underbrace{\langle E_1|E_1\rangle}_{1} - \frac{\sqrt{3}i}{4}E_2\underbrace{\langle E_1|E_2\rangle}_{0} + \frac{\sqrt{3}i}{4}E_1\underbrace{\langle E_2|E_1\rangle}_{0} + \frac{3}{4}E_2\underbrace{\langle E_2|E_2\rangle}_{1} = \frac{1}{4}E_1 + \frac{3}{4}E_2,\end{aligned}$$

or using Proposition 2:

$$\langle\psi|H|\psi\rangle = \left|\frac{1}{2}\right|^2 E_1 + \left|\frac{\sqrt{3}i}{2}\right|^2 E_2 = \frac{1}{4}E_1 + \frac{3}{4}E_2.$$

Observant readers may have spotted two potential problem with Postulate 3: First, the ket $|\psi\rangle$ is implicitly assumed to be normalized, or the total probability $\sum_n P(a_n) = \sum_n |\langle a_n|\psi\rangle|^2 = \langle\psi|\psi\rangle$ would not be unity. Second, the state-dependent probabilities $P(a_n)$ should not depend on which ket we choose to represent the state. Both of these problems are addressed by the next and last postulate of this chapter, which ensures that the probabilities are well-defined.

Postulate 4. *Two kets represent the same state iff they are scalar multiples of each other.*

Because of this postulate, kets are often assumed to be normalized and states are viewed as elements of the projective Hilbert space $\mathcal{H}/\mathbb{C}$. As stated in the beginning of this section, the terms *normalized ket* and *state* are often used interchangably despite not being equivalent since states are invariant under $U(1)$ *gauge transformations*

$$|\psi\rangle \mapsto e^{i\theta}|\psi\rangle, \qquad \theta \in \mathbb{R},$$

whilst kets are not. This is no stranger than treating a matrix as being equivalent to the basis-independent linear transformation that it represents, which is completely fine in most situations as long as one remembers the distinction. Gauge theory, essentially the study of Lie group actions on $\mathcal{H}$ that leave the underlying physics unchanged, is an important tool for extracting physics hidden within abstract mathematics.

1.2 The Schrödinger equation

Let us venture into the realm of quantum dynamics by examining how states evolve in time. It is ironic that, even though the probabilistic nature of quantum mechanics prevents us from predicting with absolute certainty the outcomes of experiments, the probabilities themselves evolve according to a deterministic equation: any state $|\psi\rangle = |\psi(t)\rangle$ satisfies the *Schrödinger equation*[6]

$$\partial_t|\psi(t)\rangle = -iH(t)|\psi(t)\rangle \tag{1.3}$$

where $H(t)$ is the Hamiltonian operator at the time t.

Example 4. Consider an arbitrary quantum system $\mathcal{H}$ with static Hamiltonian H. The energy eigenstates $|E_n\rangle$ form an orthonormal basis in $\mathcal{H}$, as per the spectral theorem, so any state $|\psi(t)\rangle$ can be written on the form

$$|\psi(t)\rangle = \sum_n \langle E_n|\psi(t)\rangle |E_n\rangle = \sum_n c_n(t)|E_n\rangle,$$

where the coordinate functions are defined as $c_n(t) := \langle E_n|\psi(t)\rangle$. By the Schrödinger equation,

$$\sum_n \dot{c}_n(t)|E_n\rangle = \partial_t|\psi(t)\rangle = -iH|\psi(t)\rangle = -i\sum_n c_n(t)H|E_n\rangle = -i\sum_n E_n c_n(t)|E_n\rangle,$$

which implies the coordinate-wise relations

$$\dot{c}_n(t) = -iE_n c_n(t), \qquad n = 1, 2, 3, \ldots.$$

These are ordinary differential equations with solutions

$$c_n(t) = c_n(0)e^{-iE_n t}, \qquad n = 1, 2, 3, \ldots,$$

[6] We set $\hbar = 1$ throughout.

hence the state can be written on the form

$$|\psi(t)\rangle = \sum_n c_n(0) e^{-iE_n t} |E_n\rangle = \sum_n e^{-iE_n t} |E_n\rangle \langle E_n|\psi(0)\rangle =: U(t) |\psi(0)\rangle ,$$

since $c_n(0) = \langle E_n|\psi(0)\rangle$. Note that the *time-evolution operator*

$$U(t) = \sum_n e^{-iE_n t} |E_n\rangle \langle E_n| = e^{-iHt}$$

is independent of the initial state $|\psi(0)\rangle$.

The time-evolution operator $U(t)$ is among the most important mathematical objects in the study of Floquet topological insulators but it is much more difficult to construct for time-dependent Hamiltonians $H(t)$ than for static ones, as both energies and instantaneous eigenstates now depend on time as well. The rest of this section is devoted to its construction as well as its properties.

Begin by observing that the Schrödinger equation (1.3) can be rewritten on the form

$$\partial_t U(t) |\psi(0)\rangle = -iH(t)U(t) |\psi(0)\rangle ,$$

for any choice of initial state $|\psi(0)\rangle$, so the time-evolution operator must satisfy the equation

$$\partial_t U(t) = -iH(t)U(t) \tag{1.4}$$

with initial condition $U(0) = \mathbb{1}$. The time-evolution operator is constructed by solving Eq. (1.4) and because of the similarity between this equation and the standard ODE for exponential growth, we expect the solution to be an exponential operator on the form

$$U(t) = e^{-i\int_0^t H(s)\ ds}.$$

Indeed, this is precisely what we found in the case of a static system in Example 4. The time-evolution operator of a more general system will turn out to be an infinite series that behaves similarly to the above exponential operator, but the two will not be equal.

By choosing a basis and integrating both sides of Eq. (1.4) element-wise, we obtain the relation

$$U(t) = \mathbb{1} - i\int_0^t H(t_1)U(t_1)\ \mathrm{d}t_1 \tag{1.5}$$

which may be iteratively expanded by writing $U(t_1)$ in terms of Eq. (1.5):

$$\begin{aligned} U(t) &= \mathbb{1} - i\int_0^t H(t_1)\left[\mathbb{1} - i\int_0^{t_1} H(t_2)U(t_2)\ \mathrm{d}t_2\right]\mathrm{d}t_1 = \\ &= \mathbb{1} + (-i)\int_0^t H(t_1)\ \mathrm{d}t_1 + (-i)^2\int_0^t H(t_1)\int_0^{t_1} H(t_2)U(t_2)\ \mathrm{d}t_2\mathrm{d}t_1. \end{aligned} \tag{1.6}$$

The last term can be simplified, as matrix multiplication and element-wise integration commutes:

$$H(t_1)\int_0^{t_1} H(t_2)U(t_2)\ \mathrm{d}t_2 = \int_0^{t_1} H(t_1)H(t_2)U(t_2)\ \mathrm{d}t_2,$$

a straightforward consequence of the fact that the matrix elements $H_{ij}(t_1)$ are independent of the integration variable t_2. Eq. (1.6) for $U(t)$ can therefore be rewritten as

$$U(t) = \mathbb{1} + (-i)\int_0^t H(t_1)\ \mathrm{d}t_1 + (-i)^2\int_0^t\int_0^{t_1} H(t_1)H(t_2)U(t_2)\ \mathrm{d}t_2\mathrm{d}t_1,$$

and we expand this formula iteratively, using Eq. (1.5), to obtain the formal power series

$$U(t) = \mathbb{1} + \sum_{n=1}^{\infty} (-i)^n \int_0^t \int_0^{t_1} \cdots \int_0^{t_{n-1}} H(t_1) \cdots H(t_n) \, \mathrm{d}t_n \cdots \mathrm{d}t_1. \tag{1.7}$$

Everything on the right-hand side can in principle be calculated so it is not necessary to proceed beyond this point, but we shall try to find a more elegant expression for $U(t)$. To this end, note that the n'th integral in Eq. (1.7) is taken over the set[7]

$$[0,t]^n_\sigma = \left\{ (t_1, \ldots, t_n) \in [0,t]^n : t_{\sigma(1)} \geq \cdots \geq t_{\sigma(n)} \right\}, \qquad \sigma \in S_n, \tag{1.8}$$

for $\sigma = e$, in which the time-variables are arranged in (right to left) chronological order. Because products of operators act from right to left, the integrand $H(t_1) \cdots H(t_n)$ is chronologically ordered, too. This enables us to rewrite Eq. (1.7) by introducing a *time-ordering operator* $\mathcal{T}$ that gives chronological order a higher priority than left-right order in products of time-dependent operators: given a product $A(t_1)B(t_2)$, we set

$$\mathcal{T}\{A(t_1)B(t_2)\} = \begin{cases} A(t_1)B(t_2), & t_1 \geq t_2 \\ B(t_2)A(t_1) & t_1 < t_2 \end{cases},$$

with the obvious extension to products of more than two operators. The time-ordering operator allows us to calculate the integral

$$\int_{[0,t]^n} \mathcal{T}\{H(t_1) \cdots H(t_n)\} \, \mathrm{d}t_n \cdots \mathrm{d}t_1$$

as a sum of $n!$ integrals with time-ordered integrands:

$$\begin{aligned} \int_{[0,t]^n} \mathcal{T}\{H(t_1) \cdots H(t_n)\} \, \mathrm{d}t_n \cdots \mathrm{d}t_1 &= \sum_{\sigma \in S_n} \int_{[0,t]^n_\sigma} H(t_{\sigma(1)}) \cdots H(t_{\sigma(n)}) \, \mathrm{d}t_n \cdots \mathrm{d}t_1 \\ &= n! \int_{[0,t]^n_e} H(t_1) \cdots H(t_n) \, \mathrm{d}t_n \cdots \mathrm{d}t_1. \end{aligned}$$

The last equality follows because each of the $n!$ integrals coincide, which can be seen by relabeling the integration variables and the order of integration. We may therefore rewrite Eq. (1.7) as

$$U(t) = \mathbb{1} + \sum_{n=1}^{\infty} \frac{(-i)^n}{n!} \int_{[0,t]^n} \mathcal{T}\left\{H(t_1) \cdots H(t_n)\right\} \mathrm{d}t_n \cdots \mathrm{d}t_1. \tag{1.9}$$

By pretending that $\mathcal{T}$ can be factored outside the infinite series, which is nothing more than abuse of notation, it is even possible to write the time-evolution operator on exponential form:

$$\begin{aligned} U(t) &= \mathbb{1} + \mathcal{T} \sum_{n=1}^{\infty} \frac{(-i)^n}{n!} \int_{[0,t]^n} H(t_1) \cdots H(t_n) \, \mathrm{d}t_n \cdots \mathrm{d}t_1 = \\ &= \mathbb{1} + \mathcal{T} \sum_{n=1}^{\infty} \frac{(-i)^n}{n!} \left(\int_0^t H(t_1) \, \mathrm{d}t_1 \right) \cdots \left(\int_0^t H(t_n) \, \mathrm{d}t_n \right) = \\ &= \mathcal{T} \sum_{n=0}^{\infty} \frac{(-i)^n}{n!} \left(\int_0^t H(s) \, \mathrm{d}s \right)^n = \mathcal{T} e^{-i \int_0^t H(s) \, \mathrm{d}s}. \end{aligned}$$

[7] Here, S_n denotes symmetric group of n elements. The n-cube $[0,t]^n$ can be split into $n!$ equally sized, triangular sections defined by the relations $t_{\sigma(1)} \geq \cdots \geq t_{\sigma(n)}$, so that $[0,t]^n = \bigcup_{\sigma \in S_n} [0,t]^n_\sigma$.

Writing $U(t) = \mathcal{T} e^{-i \int_0^t H(s)\ \mathrm{d}s}$ for the time-evolution operator is convenient, though misleading, and highlights the fact that $U(t)$ often *does* behave similarly to an exponential operator. On the other hand, one must not forget about the abuse of notation; calculations involving $U(t)$ should be conducted using a power series representation such as Eq. (1.7) or Eq. (1.9).

Remark 2. If the Hamiltonian happens to commute with itself at different times, meaning that the commutator $\big[H(t_1), H(t_2)\big]$ vanishes for all times t_1, t_2, then the time-ordering operator need not be invoked and the time-evolution operator $U(t)$ truly becomes an exponential operator:

$$U(t) = e^{-i \int_0^t H(s)\ \mathrm{d}s}.$$

We summarize the above construction in the form of a theorem.

Theorem 1. *The time-evolution operator is given by*

$$U(t) = \mathcal{T} e^{-i \int_0^t H(s)\ ds} = \mathbb{1} + \sum_{n=1}^{\infty} (-i)^n \int_0^t \int_0^{t_1} \cdots \int_0^{t_{n-1}} H(t_1) \cdots H(t_n)\ dt_1 \cdots dt_n.$$

1.2.1 Properties of the time-evolution operator

Now that we have constructed $U(t)$, let us look at some of its properties, starting with convergence. The Hamiltonian is an element of the space $\mathcal{B}(\mathcal{H})$ of bounded linear operators on the N-dimensional Hilbert space $\mathcal{H}$, and we equip $\mathcal{B}(\mathcal{H})$ with the norm

$$\|A\| = N \max_{i,j} |A_{ij}|, \qquad A \in \mathcal{B}(\mathcal{H}),$$

given some fixed basis for $\mathcal{H}$; convergence in this norm will imply convergence in any norm as all norms on the finite-dimensional space $\mathcal{B}(\mathcal{H})$ are equivalent [10]. We chose this particular norm because it implies both the Schwarz inequality

$$\|AB\| \leq \|A\| \|B\|, \qquad A, B \in \mathcal{B}(\mathcal{H}), \tag{1.10}$$

and the triangle inequality for integrals,

$$\left\| \int_0^t A(s)\ \mathrm{d}s \right\| \leq \int_0^t \|A(s)\|\ \mathrm{d}s, \tag{1.11}$$

for all integrable, time-dependent operators $A(t)$.

Theorem 2. *If the Hamiltonian $H(t)$ is continuous in time, the time-evolution operator*

$$U(t) = \mathcal{T} e^{-i \int_0^t H(s)\ ds} = \mathbb{1} + \sum_{n=0}^{\infty} (-i)^n \int_0^t \int_0^{t_1} \cdots \int_0^{t_{n-1}} H(t_1) \cdots H(t_n)\ dt_n \cdots dt_1$$

converges uniformly in $[0, T]$ for any $T \geq 0$.

Proof. By the continuity of $H(t)$ and the inverse triangle inequality,

$$\big| \|H(t+\epsilon)\| - \|H(t)\| \big| \leq \|H(t+\epsilon) - H(t)\| \to 0, \qquad \epsilon \to 0,$$

so the norm $\|H(t)\|$ is a continuous function of time and therefore attains a maximum C_T on every compact time-interval $[0, T]$:

$$C_T := \max_{t \in [0,T]} \|H(t)\|.$$

Denoting by $S_N(t)$ the partial sum[8]

$$S_N(t) = \mathbb{1} + \sum_{n=0}^{N} (-i)^n \int_0^t \int_0^{t_1} \cdots \int_0^{t_{n-1}} H(t_1) \cdots H(t_n) \, \mathrm{d}t_n \cdots \mathrm{d}t_1,$$

and applying the inequalities (1.10) & (1.11), we find that

$$\begin{aligned} \|S_N(t) - S_M(t)\| &= \left\| \sum_{n=M+1}^{N} \int_0^t \int_0^{t_1} \cdots \int_0^{t_{n-1}} H(t_1) \cdots H(t_n) \, \mathrm{d}t_n \cdots \mathrm{d}t_1 \right\| \leq \\ &\leq \sum_{n=M+1}^{N} \int_0^t \int_0^{t_1} \cdots \int_0^{t_{n-1}} \|H(t_1)\| \cdots \|H(t_n)\| \, \mathrm{d}t_n \cdots \mathrm{d}t_1 \leq \\ &\leq \sum_{n=M+1}^{N} C_T^n \left[\int_0^t \int_0^{t_1} \cdots \int_0^{t_{n-1}} 1 \, \mathrm{d}t_n \cdots \mathrm{d}t_1 \right] = \sum_{n=M+1}^{N} \frac{C_T^n t^n}{n!} \leq \sum_{n=M+1}^{N} \frac{C_T^n T^n}{n!}, \end{aligned}$$

which tends to 0 as $M, N \to \infty$, independently of $t \in [0, T]$. The partial sum $S_N(t)$ thus forms a Cauchy sequence in N that converges uniformly in the Banach space $\mathcal{B}(\mathcal{H})$. □

Corollary 2. *If the Hamiltonian $H(t)$ is continuous in time, the time-evolution operator $U(t)$ is uniformly continuous in $[0, T]$ for all $T \geq 0$.*

Proof. The uniform convergence of $U(t)$ in $[0, T]$ implies that, for every $\epsilon > 0$, there exists a natural number $N_{\epsilon,T}$ such that $\|U(t) - S_N(t)\| < \epsilon/3$ for all $N > N_{\epsilon,T}$ and all $t \in [0, T]$. Consequently,

$$\|U(t+\delta) - U(t)\| \leq \underbrace{\|U(t+\delta) - S_N(t+\delta)\|}_{<\epsilon/3} + \|S_N(t+\delta) - S_N(t)\| + \underbrace{\|S_N(t) - U(t)\|}_{<\epsilon/3} < \epsilon$$

for small enough δ, the partial sum $S_N(t)$ clearly being continuous in time. We conclude that $U(t)$ is continuous, thus also uniformly continuous, on the compact interval $[0, T]$. □

The above results were proven for finite time intervals $[0, T]$ but the parameter T can be chosen freely and is in that sense unimportant, so we do not always mention the parameter T explicitly.

Proposition 3. *The time-evolution operator $U(t)$ is unitary for all times.*

Proof. We need to show that[9]

$$U(t)^\dagger U(t) = \mathbb{1}$$

for all times $t \geq 0$, a property that is trivially true for $U(0) = \mathbb{1}$. It suffices to prove that $U^\dagger U$ is time-independent, which follows from the Schrödinger equation $\partial_t U = -iHU$ combined with the observation that differentiation commutes with taking the conjugate transpose:

$$\partial_t\big(U^\dagger U\big) = \big(\partial_t U\big)^\dagger U + U^\dagger\big(\partial_t U\big) = \big(-iHU\big)^\dagger U + U^\dagger\big(-iHU\big) = iU^\dagger HU - iU^\dagger HU = 0.$$

□

[8] The subscript N denotes an arbitrary natural number, as is standard when discussing convergence of sequences, and should not be confused with the dimension $\dim \mathcal{H} = N$.

[9] We do not need to prove that $U(t)U(t)^\dagger = \mathbb{1}$ since left- and right-inverses of finite-dimensional operators coincide.

These results show that $U(t)$ behaves nicely despite its rather ugly appearence; messing with the time-ordering might be the only way to make the time-evolution operator behave badly. Translations $t \mapsto t + t_0$, for example, preserve time-ordering and are perfectly valid, allowing us to define time-evolution starting from an arbitrary reference time t':

$$U(t, t') := \mathcal{T} e^{-i \int_{t'}^{t} H(s) \, \mathrm{d}s}.$$

We end this chapter by proving that time can be evolved in successive steps.

Proposition 4. *The time-evolution operator $U(t) = U(t, 0)$ satisfies*

$$U(t, 0) = U(t, t')U(t', 0) \tag{1.12}$$

for all finite times $t \geq t' \geq 0$.

Proof. By choosing a basis for $\mathcal{H}$ and writing linear operators on matrix-form, the equation

$$\begin{cases} \partial_t V(t) = -iH(t)V(t), & T > t > t' \\ V(t') = U(t', 0) \end{cases} \tag{1.13}$$

defines a linear system of first-order differential equations on the open interval $T > t > t' \geq 0$. Such systems are known to have unique solutions, but Eq. (1.13) is satisfied by both

$$V_1(t) = U(t, 0), \qquad \text{and} \qquad V_2(t) = U(t, t')U(t', 0),$$

so the two operators must agree:

$$U(t, 0) = U(t, t')U(t', 0), \qquad T > t \geq t'.$$

As the final time $T > t'$ can be chosen arbitrarily large, the proposition follows. □

2

Topological Materials

In this chapter, we introduce basic tools needed for mathematical analysis of topological crystalline materials. We begin with a discussion about crystal lattices, reciprocal lattices, crystal momentum and the (first) Brillouin zone, before giving a mathematical introduction to band theory. Next, we cover a number of important concepts such as the Berry phase, connection, and curvature, as well as Chern numbers and their relation to the quantized Hall conductance in the QHE. The chapter ends with a discussion about the classification of topological insulators and superconductors according to different symmetries, which is the topic of our next and final chapter.

2.1 Crystalline lattices and the Brillouin zone

Metals, semiconductors, and many other important kinds of materials in condensed matter physics and chemistry are *crystalline*, meaning that they consist of atoms or molecules arranged in highly symmetric periodic arrangements called *lattices* (Figure 2.1). Crystalline materials have been extensively studied over the past two centuries as they are ubiquitous, easy to model, and have an enormous number of interesting applications.

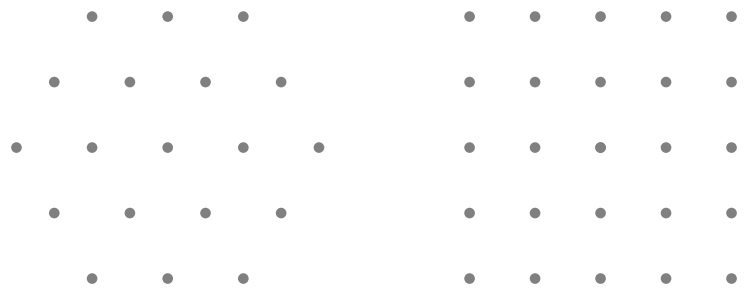

(a) Hexagonal lattice **(b)** Square lattice

Figure 2.1: Two different 2-dimensional Bravais lattices.

Since the discovery of the quantum Hall effect and robust edge currents, physicists have also become interested in the *topological* properties of crystals, an interest that has only grown as more and more materials with such properties have been discovered. Topological phenomena have been studied in the contexts of several important research areas, including superconductors, semimetals,

and quantum computation. When designing a quantum computer, for example, a main problem has been designing information-storing qubits that are insensitive to the effects of decoherence, i.e. destructive interaction with the environment that results in information loss. One way to solve this problem would be to design qubits using topologically protected stationary states located at the edges of a 1D topological quantum wire.

Definition. Given a basis $a_1, \dots, a_d$ for $\mathbb{R}^d$, the set

$$\mathcal{B}_a = \{n_1 a_1 + \cdots + n_d a_d \mid n_1, \dots, n_d \in \mathbb{Z}\}$$

is called a d-dimensional *Bravais lattice*, or simply a *lattice*. The elements of a Bravais lattice are called *lattice vectors*, or *sites*, and the *primitive* vectors $a_1, \dots, a_d$ are said to *generate* the lattice.

The number of atoms in a typical crystal is so large, and interactions between distant particles so small, that it makes no practical difference whether the crystal is finite or infinite when studying particles located deep inside the crystal bulk. Infinite Bravais lattices are thus good approximations of real crystals. Nevertheless, the crystal boundary has to be taken into consideration at some point and will become increasingly important as we go along.

Given an arbitrary lattice $\mathcal{B}_a$, we can construct a *reciprocal* lattice $\mathcal{B}_b$ through the requirement that $a_i \cdot b_j = 2\pi\delta_{ij}$ for each pair of primitive vectors $a_i \in \mathcal{B}_a$ and $b_j \in \mathcal{B}_b$. If the sites in one lattice represent positions of ions or molecules in physical space, then the sites in the reciprocal lattice represent *crystal momentum*, a discrete analogue of ordinary momentum. Lattice position and crystal momentum are basically discrete Fourier transforms of each other, just as ordinary position and momentum are related by a continuous Fourier transform[1].

Proposition 5. *If $\mathcal{B}_a$ is a 2-dimensional Bravais lattice generated by the primitive vectors*

$$a_1 = a\begin{pmatrix}\cos\theta_1\\ \sin\theta_1\end{pmatrix}, \qquad a_2 = a\begin{pmatrix}\cos\theta_2\\ \sin\theta_2\end{pmatrix},$$

for some lattice constant $a > 0$, then its reciprocal lattice $\mathcal{B}_b$ is generated by the primitive vectors

$$b_1 = \frac{2\pi}{a\sin(\theta_2-\theta_1)}\begin{pmatrix}\sin\theta_2\\ -\cos\theta_2\end{pmatrix}, \qquad b_2 = \frac{2\pi}{a\sin(\theta_2-\theta_1)}\begin{pmatrix}-\sin\theta_1\\ \cos\theta_1\end{pmatrix}.$$

Proof. It suffices to check that $a_i \cdot b_j = 2\pi\delta_{ij}$ for $i, j = 1, 2$, a straightforward task. □

Example 5. A uniform grid of mutually identical ions defines a translationally invariant Bravais lattice with one ion per lattice site. If we assume the lattice to be perfectly rigid, meaning that the ions cannot move relative to each other, a lone electron positioned at $r \in \mathbb{R}^d$ will interact with the lattice ions through the Coulomb potential

$$V(r) = -\sum_i \frac{e^2}{4\pi\epsilon_0}\frac{1}{\|r - R_i\|_2},$$

[1] The position operator $\mathbf{x}$ in an infinite-dimensional 1D system $\mathcal{H} = L^2(\mathbb{R})$ is given by multiplication by x whilst the momentum operator is given by $\mathbf{p} = -i\partial_x$. The roles of these operators can be switched by letting them act on an arbitrary Schwartz class function $\psi \in \mathcal{H}$ and applying a Fourier transform:

$$\widehat{\mathbf{p}\psi} = -i\int_{-\infty}^{\infty} \partial_x\psi(x)e^{-ipx}\,\mathrm{d}x = i\int_{-\infty}^{\infty}\psi(x)\partial_x e^{-ipx}\,\mathrm{d}x = p\int_{-\infty}^{\infty}\psi(x)e^{-ipx}\,\mathrm{d}x = p\hat{\psi}(p),$$

a similar calculation yielding $\widehat{\mathbf{x}\psi} = -i\partial_p\hat{\psi}(p)$. The position and momentum operators in $\mathcal{H}$ are thus distributional Fourier transforms of each other, as the Schwartz class is dense in $L^2(\mathbb{R})$, and analogous versions of this result can be shown in other quantum systems.

the lattice vector $R_i \in \mathcal{B}_a$ denoting the fixed position of the i'th ion. The electron cannot possibly know where it is located inside this infinite, translationally invariant lattice, so moving the electron to a different region should have no effect on its dynamics. In other words, we expect the Coulomb potential to inherit the translational symmetry of the lattice. Indeed,

$$\begin{aligned} V(r+R_j) &= -\sum_i \frac{e^2}{4\pi\epsilon_0}\frac{1}{\|r+R_j-R_i\|_2} = \left[R_{i'} := R_i - R_j\right] = \\ &= -\sum_{i'} \frac{e^2}{4\pi\epsilon_0}\frac{1}{\|r-R_{i'}\|_2} = V(r), \end{aligned}$$

for each lattice site $R_j \in \mathcal{B}_a$.

The above example illustrates an important fact, namely that a fairly large number of physical properties and phenomena share the translational invariance of the lattice. Crystalline materials can therefore be studied by restricting attention to a suitable neighbourhood inside the crystal, such as a Wigner-Seitz cell.

Definition. Let $\mathcal{B}_a$ be a d-dimensional Bravais lattice. The *Wigner-Seitz cell* around a site R is the locus of points in $\mathbb{R}^d$ with shorter distance to R than to any other site R':

$$\mathcal{WS}(R) := \left\{ r \in \mathbb{R}^d \;\middle|\; \min_{R' \in \mathcal{B}_a} \|r-R'\|_2 = \|r-R\|_2 \right\}.$$

The Wigner-Seitz cell around $k=0$ in reciprocal space is called the *(first) Brillouin zone*.

Different Wigner-Seitz cells are clearly related by translation,

$$\mathcal{WS}(R') = \mathcal{WS}(R) + R' - R,$$

and together they tile $\mathbb{R}^d$. Local physics look the same in one cell as it does in any other cell, so we might as well identify different cells with each other by defining an equivalence relation

$$r \sim r' \qquad \Longleftrightarrow \qquad r' - r \in \mathcal{B}_a$$

and moving to the quotient $\mathcal{WS}(0)/\sim$.

Example 6. The square Bravais lattice in Figure 2.1b is generated by the primitive vectors

$$a_1 = a\begin{pmatrix}1\\0\end{pmatrix}, \qquad a_2 = a\begin{pmatrix}0\\1\end{pmatrix}.$$

Its reciprocal lattice is therefore the square lattice generated by

$$b_1 = \frac{2\pi}{a}\begin{pmatrix}1\\0\end{pmatrix}, \qquad b_2 = \frac{2\pi}{a}\begin{pmatrix}0\\1\end{pmatrix},$$

with (first) Brillouin zone

$$BZ = \mathcal{WS}(k=0) = \left[-\frac{\pi}{a}, \frac{\pi}{a}\right] \times \left[-\frac{\pi}{a}, \frac{\pi}{a}\right].$$

Both quotient spaces $\mathbb{R}^2/\sim$ and $BZ/\sim$ are homeomorphic to the 2-torus $\mathbb{T}^2 = S^1 \times S^1$.

Topological insulators and other solid state systems are often studied by looking at the dynamics of a single electron moving in a lattice devoid of other electrons, as the resulting theory can then be applied to each electron in a non-interacting system. It may seem strange to assume that electrons do not interact with each other, but it leads to a significantly simpler theory that still manages to correspond well with experiments in a large number of situations. The assumption can even be justified from a theoretical standpoint, as the Pauli exclusion principle and screening of the Coulomb interaction significantly reduces the likelihood of collisions between electrons [18]. Furthermore, electron-electron interactions can always be taken into consideration later on as a correction to the non-interacting theory. We will therefore focus on single-particle Hamiltonians.

To be precise, our focus will be on crystalline materials in two spatial dimensions, described by a single-particle *bulk momentum-space* Hamiltonian $H(k)$ in an N-dimensional quantum system. The crystal momenta $k = (k_x, k_y)$ are assumed to live inside a square Brillouin zone

$$BZ = [-\pi, \pi] \times [-\pi, \pi]$$

that we often identify with the 2-torus.

2.2 Band theory

Given an arbitrary Hamiltonian $H = H(x)$ that depends on some real parameter x, representing for example time and crystal momentum, we want to understand what happens to each individual energy eigenvalue $E_n(x)$ as the parameter x is varied. This simple question is surprisingly difficult to answer in general, an important point that we will soon talk more about, but some conclusions can be drawn. A good start is that continuity of $H(x)$ implies continuity in the spectral metric [16]

$$d(H(x), H(x')) = \min_{\sigma \in S_N} \max_n |E_n(x) - E_{\sigma(n)}(x')| \tag{2.1}$$

that provides a meaningful distance between the spectrum of $H(x)$ and that of $H(x')$.

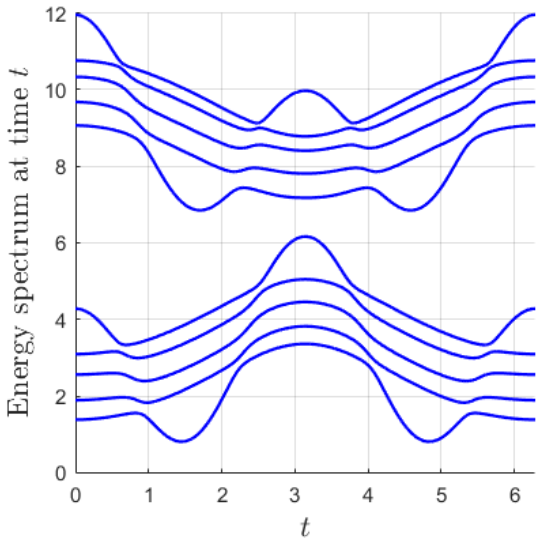

Figure 2.2: The spectrum of a continuously time-dependent Hamiltonian $H(t)$ can be considered a (multivalued) continuous function of time. Its graph is known as the *energy band structure*.

The band structure is informally defined as the graph of the spectrum of $H(x)$. As the name suggests and as Figure 2.2 clearly shows, the band structure is composed of a number of *bands*, which are the individual eigenvalues $E_n(x)$ considered as continuous functions of x. The idea of bands seems natural but rigorously proving their existence and examining their properties turns out to be very difficult. The problem is that of ordering the eigenvalues: we cannot prove, say, that the difference $|E_n(x) - E_n(x')|$ vanishes alongside $|x - x'|$ unless we also know which eigenvalue is the n'th one for each parameter x' in a neighbourhood of x.

A natural choice would be to order the eigenvalues by size, i.e. to choose the ordering

$$n \geq m \qquad \text{if and only if} \qquad E_n(x) \leq E_m(x) \tag{2.2}$$

for every x. This ordering is guaranteed to produce continuous bands, as

$$|E_n(x) - E_n(x')| \leq \max_n |E_n(x) - E_n(x')| = d\big(H(x), H(x')\big),$$

due to the fact that $\sigma = e$ minimizes Eq. (2.1) for this particular ordering. It is not recommended to use this size-based ordering, however, as differentiability or higher degrees of smoothness will be lost whenever two bands cross. The bands E_1 and E_2 in Figure 2.3, for example, are defined using Eq. (2.2) but it would clearly have been better to set $E_1(x) = \cos(x)$ and $E_2(x) = \sin(x)$.

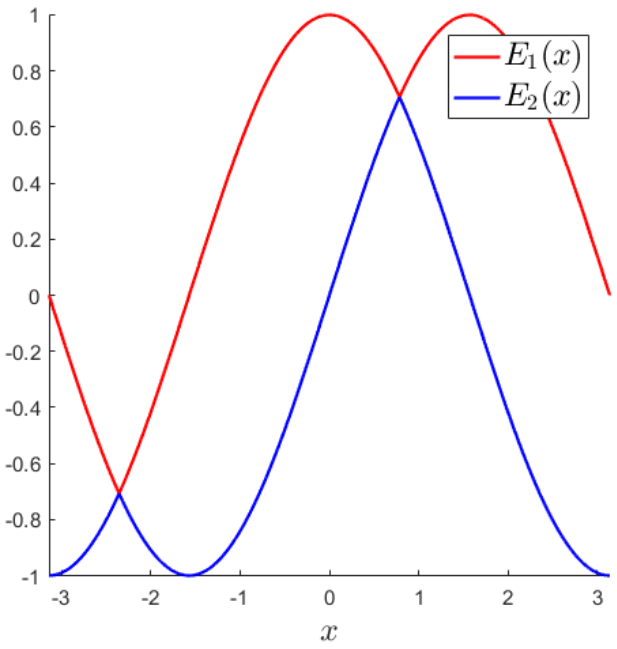

Figure 2.3: Bands constructed using Eq. (2.2) are continuous but rarely differentiable.

Another problem is that bands do not always inherit smoothness from the Hamiltonian, as illustrated in the following example by the legendary Kato [16].

Example 7. The Hermitian operator

$$H(x_1, x_2) = \begin{pmatrix} x_1 & x_2 \\ x_2 & -x_1 \end{pmatrix}$$

is totally differentiable in x_1, x_2 and diagonalizable for all real numbers x_1, x_2, but its eigenvalues

$$E_\pm(x_1, x_2) = \pm\sqrt{x_1^2 + x_2^2}$$

are not totally differentiable at $x_1 = x_2 = 0$.

At this point, it should be clear that band theory can be subtle and tricky. Fortunately, some regularity can still be guaranteed for most physically relevant operators [16].

Kato's theorem. *Let $A = A(x)$ be a linear operator on an N-dimensional complex Hilbert space, defined for $x \in [0,1]^d$. Denote by $\mathfrak{S}(x)$ the unordered N-tuple of eigenvalues $a_n(x)$ of $A(x)$:*

$$\mathfrak{S}(x) = \big(a_1(x), \dots, a_N(x)\big), \qquad x \in [0,1]^d.$$

If the operator A is continuous on $[0,1]^d$, then there exists N continuous functions

$$A_n : [0,1]^d \to \mathbb{C}, \qquad n = 1, \dots, N,$$

such that

$$\mathfrak{S}(x) = \big(A_1(x), \dots, A_N(x)\big), \qquad x \in [0,1]^d.$$

In other words, the full spectrum of A can be split into N continuous bands A_n. If the operator $A(x)$ is diagonalizable and partially differentiable, and if the unordered N-tuple $\mathfrak{S}(x)$ is differentiable[2], then the bands A_n are also partially differentiable.

Both Hermitian and unitary operators are diagonalizable, and differentiability of $\mathfrak{S}(x)$ can often be justified. Kato's theorem therefore applies to a large number of observables, the time-evolution operator, and many other operators that arise naturally in quantum mechanics. Furthermore, most of the Hamiltonians one encounters in practice are highly regular so we may assume partial differentiability without significantly restricting our theory. Observe that the time-evolution operator inherits partial differentiability from the Hamiltonian.

We now know that the energy of any electron in a non-interacting system lies inside an energy band, but not all energies are equally probable, the electron will most often be found in the lowest energy state called the *quantum ground state*. Furthermore, the Pauli exclusion principle dictates that no pair of electrons can occupy the same state, so adding more electrons to the system has the effect of filling up the avaliable energies from the bottom up; the M-particle ground state is then defined as the state in which the M lowest energies of the single-particle Hamiltonian are filled. These ideas can be expressed mathematically using the framework of *second quantization*, which we shall discuss in the next chapter. For example, *creation* and *annihilation operators* $c_{nk}^\dagger$ and c_{nk} are used to create or annihilate an electron at crystal momentum k in the n'th energy band.

The number of electrons in a system is more or less constant, so the ground state is often well-defined and so is the *Fermi level* E_F that measures the work required to add another electron

[2] $\mathfrak{S}(x)$ is differentiable at a point x if it can be represented in a neighbourhood of x by N functions $\mu_1, \dots, \mu_N$ which are differentiable at x. This is a relatively weak assumption since $\mathfrak{S}(x) = \big(\mu_1(x), \dots, \mu_N(x)\big)$ is unordered.

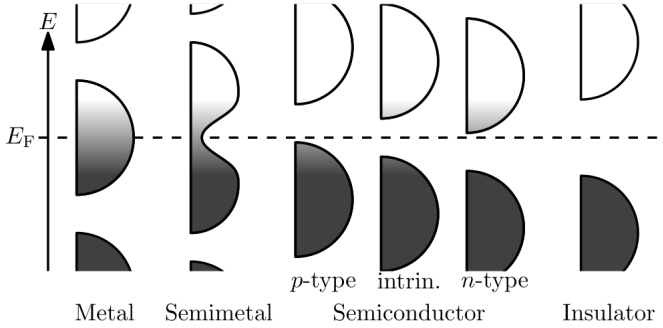

Figure 2.4: The electrical properties of a crystalline material depends on the location of the Fermi level E_F in relation to the energy bands. If the Fermi level lies inside a band, electrons are easily excited and the system becomes metallic; if the Fermi level lies inside a large band gap, excitations are rare and the system becomes insulating. Here, "width is the density of available states for a certain energy in the material listed" [38].

to the system. Crystalline materials are categorized as metals, semimetals, semiconductors, and insulators, according to the position of the Fermi level in relation to the energy bands (Figure 2.4). Indeed, electrical conduction is a manifestation of electrons jumping between different energy states and every energy state below the Fermi energy is occupied, whilst every energy state above the Fermi level is unoccupied, so the position of the Fermi level is an indication of the ease with which electrons can be excited. If the Fermi level lies inside an energy band, for example, an electron near the Fermi level can easily be excited to higher energy states (inside the same band), leading to good electrical properties. If the Fermi level lies in the middle of a sizeable band gap, on the other hand, electrons are rarely excited and the electrical properties are poor; the system is insulating. We are interested in insulating band structures so the Fermi level is assumed to lie at the center of a sizeable band gap, and all energies are assumed to be rescaled so that $E_F = 0$.

Curiously, superconductors also have an insulating band structure and are therefore included in our analysis. What happens in a superconductor is that vibrations in the crystal lattice induce an attractive interaction between electrons, causing some of the electrons near the Fermi energy and with opposite crystal momentum $\pm k$ to pair up. The collective behaviour of such a *Cooper pair* is that of a single bosonic[3] quasiparticle and since bosons are unaffected by the Pauli principle, there is nothing to prevent all of the Cooper pairs from condensing into the same ground state, a process that lowers the energy of each paired electron and creates an energy gap between these and normal electrons. This gap does not prevent conduction like in an insulator, but *protects* the current-carrying Cooper pairs from interactions which normally cause resistivity. The current is therefore allowed to flow freely, without resistance.

We end this section with an important result about time-dependent quantum systems.

Adiabatic theorem. *A quantum system can be changed over time without disturbing the state, provided that the change occurs slowly enough. In other words, the probability density function*

$$P(E_n(t)) = |\langle E_n(t)|\psi(t)\rangle|^2$$

in a gradually changing quantum system is approximately time-independent.

[3]Particles can be categorized into bosons and fermions. Most elementary particles (e.g. electrons and protons) are fermions while the list of bosons contain photons, the Higgs boson, a number of quasiparticles such as phonons and Cooper pairs, et cetera. These two categories obey different statistics, have different spin properties, and the Pauli exclusion principle applies only to fermions.

Proof. We present a standard proof of this theorem. As the instantaneous eigenstates $|E_n(t)\rangle$ form an orthonormal basis for each time t, it is possible to write an arbitrary state $|\psi(t)\rangle$ on the form

$$|\psi(t)\rangle = \sum_m c_m(t) e^{-i\theta_m(t)} |E_m(t)\rangle, \qquad \text{where} \qquad \theta_m(t) = \int_0^t E_m(s)\, \mathrm{d}s,$$

so its time-derivative evaluates as

$$\begin{aligned}
\partial_t |\psi(t)\rangle &= \sum_m e^{-i\theta_m(t)} \Big(\dot{c}_m(t) - i c_m(t)\dot{\theta}_m(t) + c_m(t)\partial_t \Big) |E_m(t)\rangle = \\
&= \sum_m e^{-i\theta_m(t)} \Big(\dot{c}_m(t) + c_m(t)\partial_t \Big) |E_m(t)\rangle - i \sum_m c_m(t) e^{-i\theta_m(t)} E_m(t) |E_m(t)\rangle = \\
&= \sum_m e^{-i\theta_m(t)} \Big(\dot{c}_m(t) + c_m(t)\partial_t \Big) |E_m(t)\rangle - iH(t) |\psi(t)\rangle .
\end{aligned}$$

By Schrödinger, $\partial_t |\psi(t)\rangle = -iH(t)|\psi(t)\rangle$ so the two remaining terms cancel each other out:

$$\sum_m \dot{c}_m(t) e^{-i\theta_m(t)} |E_m(t)\rangle = -\sum_m c_m(t) e^{-i\theta_m(t)} \big|\dot{E}_m(t)\big\rangle ,$$

where $\big|\dot{E}_m(t)\big\rangle := \partial_t |E_m(t)\rangle$. Left-multiplication by $\langle E_n(t)|$ therefore yields the relation

$$\dot{c}_n(t) = -\sum_m c_m(t) e^{-i\left(\theta_m(t) - \theta_n(t)\right)} \big\langle E_n(t)\big|\dot{E}_m(t)\big\rangle .$$

Now observe that if m and n correspond to different energies, $E_m(t) \neq E_n(t)$, then

$$0 = \partial_t \langle E_n(t)|H(t)|E_m(t)\rangle = \underbrace{\big\langle \dot{E}_n(t)\big|H(t)\big|E_m(t)\big\rangle}_{E_m(t)\big\langle \dot{E}_n(t)\big|E_m(t)\big\rangle} + \langle E_n(t)|\dot{H}(t)|E_m(t)\rangle + \underbrace{\big\langle E_n(t)\big|H(t)\big|\dot{E}_m(t)\big\rangle}_{E_n(t)\big\langle E_n(t)\big|\dot{E}_m(t)\big\rangle}$$

and in a similar way, the identity $\partial_t \langle E_n(t)|E_m(t)\rangle = \partial_t \delta_{mn} = 0$ implies the relation

$$\big\langle \dot{E}_n(t)\big|E_m(t)\big\rangle = -\langle E_n(t)|\, \dot{E}_m(t). \tag{2.3}$$

Combining the two equations above, we obtain the expression

$$\big\langle E_n(t)\big|\dot{E}_m(t)\big\rangle = \frac{\langle E_n(t)|\dot{H}(t)|E_m(t)\rangle}{E_n(t) - E_m(t)} \qquad (m \neq n)$$

which holds whenever the energy eigenvalue $E_n(t)$ is a simple eigenvalue. The time-derivative $\dot{c}_n(t)$ can then be written on the form

$$\dot{c}_n(t) = -c_n(t) \big\langle E_n(t)\big|\dot{E}_n(t)\big\rangle - \sum_{m\neq n} c_m(t) \frac{\langle E_n(t)|\dot{H}(t)|E_m(t)\rangle}{E_n(t) - E_m(t)} e^{-i\left(\theta_m(t) - \theta_n(t)\right)}.$$

If the system changes gradually enough, in the sense that $\dot{H}(t)$ is small compared to the energy differences $E_n(t) - E_m(t)$, then the second term becomes negligible and we conclude that

$$c_n(t) \approx c_n(0) e^{-\int_0^t \big\langle E_n(s)\big|\dot{E}_n(s)\big\rangle \, \mathrm{d}s}.$$

The inner product $\langle E_n(t)|\dot{E}_n(t)\rangle$ is purely imaginary by Eq. (2.3), so the initial coefficient $c_n(0)$ only changes by a phase factor and the time-dependent probability distribution

$$P(E_n(t)) = |\langle E_n(t)|\psi(t)\rangle|^2$$

becomes approximately static. In particular, a slowly changing system prepared in the n'th eigenstate

$$|\psi(0)\rangle = c_n(0)\,|E_n(0)\rangle$$

will stay in the n'th eigenstate[4]

$$|\psi(t)\rangle = c_n(t)\,|E_n(t)\rangle$$

for all times. □

2.3 Topological insulators

What distinguishes topological insulators from ordinary insulators is the existence of topologically protected *surface states*, which in the 2D case are known as *chiral edge states*. These are robust electronic channels localized to the crystal boundary and which propagate in a single direction [9], thereby allowing a stable edge current to form, just as in the quantum Hall effect. Furthermore, the chiral edge states are not eigenstates of the insulating bulk Hamiltonian $H(k)$, which is constructed under an explicit assumption (translational invariance) that fails to hold near the boundary. The *number* of chiral edge states, however, can be obtained from the bulk Hamiltonian and is invariant under adiabatic deformations; homotopies which do not close the band gap. This relation between bulk Hamiltonian and the number of chiral edge states is called the *bulk-boundary correspondence*.

The mathematical starting point is a Hamiltonian $H = H(x)$ that depends continuously on a collection of parameters, x, living inside some parameter manifold $\mathcal{M}$. In our case, x will be either crystal momentum (Chapter 2) or a combination of crystal momentum and time (Chapter 3), and the parameter manifold will be the 2-torus and the 3-torus, respectively. The basic idea is that a topologically nontrivial parameter manifold can induce topological behaviour in a material. In contrast, we would not expect to find topological behaviour in a system with topologically trivial parameter manifold such as $\mathbb{R}^n$.

2.3.1 Berry phase

Let us follow the standard approach [3, 4, 32, 33] by looking at the behaviour of an initial state

$$|\psi(x_0)\rangle = |E_n(x_0)\rangle$$

that is transported adiabatically[5] along an arbitrary curve $\mathcal{C} : [0,T] \to \mathcal{M}$, $t \mapsto x(t)$ in the parameter manifold. By the adiabatic theorem, the system will stay in the instantaneous eigenstate

$$|\psi(x(t))\rangle = e^{i\theta_n(x(t))}\,|E_n(x(t))\rangle \tag{2.4}$$

for all times, and we can find an explicit expression for θ_n through a combination of Schrödinger,

$$-iE_n\,|E_n\rangle = -iH\,|\psi\rangle = \partial_t\,|\psi\rangle = -i\frac{\partial\theta_n}{\partial t}\,|E_n\rangle + \partial_t\,|E_n\rangle\,,$$

[4] This is strictly speaking an approximation rather than an equality, but the difference is negligible to physicists.
[5] That is, slowly enough for the adiabatic theorem to apply.

and left-multiplication by $\langle E_n|$, yielding the differential equation $\frac{\partial \theta_n}{\partial t} = E_n - i \langle E_n| \partial_t |E_n\rangle$ with initial condition $\theta_n(x_0) = 0$. Integrating both sides of course gives us the exact solution

$$\theta_n(x(t)) = \int_0^t E_n(x(s))\ \mathrm{d}s - \int_0^t i \langle E_n(x(s))|\partial_t|E_n(x(s))\rangle\ \mathrm{d}s.$$

The first term on the right-hand side is the dynamical phase associated with the time-evolution and the second term is known as the *Berry phase*

$$\gamma_n(t) = \int_0^t i \langle E_n(x(s))| \partial_s |E_n(x(s))\rangle \,\mathrm{d}s.$$

States are elements of the projective Hilbert space $\mathcal{H}/\mathbb{C}$ so we are tempted to dismiss the dynamical phase and the Berry phase as being physically irrelevant, but this would be a mistake. Physical phenomena are typically insensitive to global gauge transformations $|\psi\rangle \mapsto e^{i\xi} |\psi\rangle$ for any constant scalar ξ but a phase that changes alongside the state can have cumulative, observable consequences, the prototypical example being the Berry phase $\gamma_n(\mathcal{C}) := \gamma_n(T)$ of a closed curve ($x(T) = x(0)$).

The Berry phase can be rewritten as a line integral

$$\gamma_n(\mathcal{C}) = \oint_{\mathcal{C}} \mathcal{A}^n(x) \cdot \mathrm{d}x$$

of the *Berry connection* $\mathcal{A}^n(x) = i \langle E_n(x)| \nabla_x |E_n(x)\rangle$. Applying a general gauge transformation $|\psi(x)\rangle \mapsto e^{i\xi(x)} |\psi(x)\rangle$ transforms the Berry connection by $\mathcal{A}^n(x) \mapsto \mathcal{A}^n(x) - \nabla_x \xi(x)$, hence

$$\gamma_n(\mathcal{C}) \mapsto \gamma_n(\mathcal{C}) + \xi(x(T)) - \xi(x(0)).$$

At this point, we run into a problem with multi-valuedness. Let us illustrate with an example [33].

Example 8. The negative energy eigenstate $|E_-\rangle$ of a gapped two-band model

$$H(k) = d(k) \cdot \sigma = \begin{pmatrix} d_z(k) & d_x(k) - id_y(k) \\ d_x(k) + id_y(k) & -d_z(k) \end{pmatrix}$$

can be written in spherical coordinates as[6]

$$|E_-(\phi, \theta)\rangle = \begin{pmatrix} \sin\left(\frac{\theta}{2}\right) e^{-i\phi} \\ -\cos\left(\frac{\theta}{2}\right) \end{pmatrix}.$$

This state is multi-valued at the north pole $\theta = 0$ where the azimuth ϕ is allowed to take any value and though the problem can be solved by a gauge transformation $|E_-(\phi, \theta)\rangle \mapsto e^{i\phi} |E_-(\phi, \theta)\rangle$, this just makes the state multi-valued at the south pole $\theta = \pi$ instead. It is impossible to make this state single-valued over its entire parameter manifold, no suitable gauge exists. It is possible, however, to make the state single-valued in a neighbourhood of any given point.

If we assume the state $|E_n\rangle$ to be single-valued on a closed curve $\mathcal{C}$, we can conclude that

$$e^{i\xi(T))} |E_n(T)\rangle = e^{i\xi(0)} |E_n(0)\rangle = e^{i\xi(0)} |E_n(T)\rangle$$

from which it follows that $\xi(x(T)) - \xi(x(0)) = 2\pi m$ for some integer m. In other words, the Berry phase over a closed curve is gauge invariant mod 2π and the phase factor $e^{i\gamma_n(\mathcal{C})}$ is gauge invariant.

[6] We follow the physics convention of using θ for the polar angle and ϕ for the azimuth.

Working directly with states is difficult due to problems with multi-valuedness, so we would prefer a different way to calculate the Berry phase. To this end, define the *Berry curvature* [33]

$$\mathcal{F}^n = \underbrace{\frac{1}{2}\left(\frac{\partial \mathcal{A}_j^n}{\partial x_i} - \frac{\partial \mathcal{A}_i^n}{\partial x_j}\right)}_{\mathcal{F}_{ij}^n} \mathrm{d}x^i \wedge \mathrm{d}x^j.$$

The Berry curvature can be defined globally on the manifold $\mathcal{M} = BZ$, without worrying about multi-valuedness [33]. It is also invariant under gauge transformations $|\psi(x)\rangle \mapsto e^{i\xi(x)}|\psi(x)\rangle$, since

$$\frac{\partial \mathcal{A}_j^n}{\partial x_i} \mapsto \frac{\partial\big[\mathcal{A}_j^n - \partial_j \xi(x)\big]}{\partial x_i} = \frac{\partial \mathcal{A}_j^n}{\partial x_i} - \frac{\partial^2 \xi(x)}{\partial x_i \partial x_j}$$

and the contribution from the second term vanishes:

$$\frac{\partial \mathcal{A}_j^n}{\partial x_i} - \frac{\partial \mathcal{A}_i^n}{\partial x_j} \mapsto \left(\frac{\partial \mathcal{A}_j^n}{\partial x_i} - \frac{\partial^2 \xi(x)}{\partial x_i \partial x_j}\right) - \left(\frac{\partial \mathcal{A}_i^n}{\partial x_j} - \frac{\partial^2 \xi(x)}{\partial x_j \partial x_i}\right) = \frac{\partial \mathcal{A}_j^n}{\partial x_i} - \frac{\partial \mathcal{A}_i^n}{\partial x_j}.$$

Now suppose that the state is single-valued and smooth on a surface $\mathcal{S}$ in the parameter manifold, as well as on its (positively oriented) boundary $\mathcal{C} = \partial\mathcal{S}$. Stoke's theorem then implies that

$$\oint_{\mathcal{C}} \mathcal{A}^n(x) \cdot \mathrm{d}x = \int_{\mathcal{S}} \mathcal{F}^n. \tag{2.5}$$

We have already seen that single-valuedness is a gauge dependent property so the above equality cannot be expected to hold in any other gauge, as Stoke's theorem would not be applicable. Another reason is, of course, that the line integral on the left-hand side is gauge invariant mod 2π whereas the surface integral on the right-hand side is gauge invariant full stop. What the Berry curvature offers, then, is a gauge invariant way of calculating a particular value of the Berry phase.

The Berry curvature can be globally defined on the parameter manifold $\mathcal{M} = BZ$ and can therefore be integrated over the entire manifold. Just like the famous Gauss-Bonnet theorem relates the Gaussian curvature K of a boundaryless manifold $\mathcal{M}$ to its Euler characteristic χ,

$$\frac{1}{2\pi}\int_{\mathcal{M}} K = \chi,$$

the Chern theorem relates the Berry curvature $\mathcal{F}^n$ to the *Chern number* of the n'th energy band:

$$\frac{1}{2\pi}\int_{BZ} \mathcal{F}^n = \nu_n.$$

The Chern number ν_n is an integer topological invariant that, in a sense, captures the problem with multivaluedness that we discussed above: Suppose that the state (2.4) can be made single-valued and smooth over the entire Brillouin torus BZ. Any contractible, closed curve $\mathcal{C}$ divides the torus into two surfaces $\mathcal{S}_1$ and $\mathcal{S}_2$ satisfying $\partial\mathcal{S}_1 = \partial\mathcal{S}_2 = \mathcal{C}$, and Stoke's theorem implies the relation

$$\int_{\mathcal{S}_1} \mathcal{F}^n = \oint_{\mathcal{C}} \mathcal{A}^n(x) \cdot \mathrm{d}x = -\int_{\mathcal{S}_2} \mathcal{F}^n,$$

where the minus sign on the right-hand side stems from the curve being positively oriented for one of the surfaces and negatively oriented for the other. The Chern number then equals

$$\nu_n = \frac{1}{2\pi}\int_{BZ} \mathcal{F}^n = \frac{1}{2\pi}\int_{\mathcal{S}_1} \mathcal{F}^n + \frac{1}{2\pi}\int_{\mathcal{S}_2} \mathcal{F}^n = 0.$$

Now suppose that the state can be made single-valued and smooth on $\mathcal{S}_1$ in one gauge, and on $\mathcal{S}_2$ in another gauge. Stoke's theorem can then be applied in each gauge separately to show that

$$\nu_n = \frac{1}{2\pi}\int_{BZ}\mathcal{F}^n = \frac{1}{2\pi}\int_{\mathcal{S}_1}\mathcal{F}^n + \frac{1}{2\pi}\int_{\mathcal{S}_2}\mathcal{F}^n = \frac{1}{2\pi}\underbrace{\left(\oint_{\mathcal{C}}\mathcal{A}_1^n(x)\cdot\mathrm{d}x - \oint_{\mathcal{C}}\mathcal{A}_2^n(x)\cdot\mathrm{d}x\right)}_{2\pi m} = m$$

for some integer m. This is because the Berry connections $\mathcal{A}_1$ and $\mathcal{A}_2$ are related by the gauge transformation that takes us from the gauge for $\mathcal{S}_1$ to the gauge for $\mathcal{S}_2$, so the two line integrals define the same Berry phase mod 2π. Once again, the minus sign stems from the orientation.

We now know that the Berry curvature $\mathcal{F}^n$ can be integrated over the Brillouin zone to yield an integer topological invariant ν_n, but what does this have to do with physics? In short, the quantized Hall conductance σ_H in the QHE equals[7] [28]

$$\sigma_H = -\frac{e^2}{h}\nu,$$

where

$$\nu = \sum_{n=1}^{N_-}\nu_n$$

is the sum of the Chern numbers of the occupied bands $n = 1, \ldots, N_-$.

The Berry curvature is also important for classifying the ground state, as we will explain in the following recount of references [9, 28]. The quantum ground state corresponding to a single-particle Hamiltonian $H(k)$, at some fixed crystal momentum k, can be described by the spectral projector

$$P(k) = \sum_{n=1}^{N_-}|E_n(k)\rangle\langle E_n(k)|,$$

where the sum is taken over the $N_- = N_-(k)$ occupied bands[8]. We use it to define the Q matrix

$$Q(k) = \mathbb{1} - 2P(k) = \sum_{n=1}^{N}\delta_n|E_n\rangle\langle E_n|, \qquad \delta_n = \begin{cases} -1\,, & n \le N_- \\ +1\,, & n > N_- \end{cases}$$

the eigenvalues of which are -1 for the occupied bands and $+1$ for the unoccupied bands. This unitary operator is invariant under unitary transformations of the $N_\pm$ (un)occupied bands and is therefore an element of the quotient space $U(N)/U(N_-)\times U(N_+)$. In general, the numbers $N_\pm$ depend on the choice of crystal momentum k but the only way for them to change is if at least one band crosses the Fermi level, so the presence of a sizeable band gap ensures that the numbers stay constant throughout the Brillouin zone. The Q-matrix then becomes a map

$$Q : BZ \to U(N)/U(N_+)\times U(N_-)$$

which, if continuous, allows the classification of ground states in terms of the homotopy group[9]

$$\pi_d\big(U(N)/U(N_+)\times U(N_-)\big) \simeq \begin{cases} \mathbb{Z}\,, & d \text{ even} \\ 0\,, & d \text{ odd} \end{cases}, \tag{2.6}$$

[7] We have set $\hbar = 1$, so $h = 2\pi$ in our units.
[8] Similarly, the number of unoccupied bands is denoted by $N_+(k) = N - N_-(k)$.
[9] The isomorphism holds "for large enough $N_\pm$" [9].

where d is the spatial dimension of the crystal lattice, in our case $d = 2$. A more detailed explanation of this kind of classification procedure is given in the next chapter. The homotopy class of the Q-matrix in $d = 2l$ spatial dimensions is thus characterized by an integer topological invariant, which is called the l'th Chern number and given by the integral

$$\mathrm{Ch}_l = -\frac{1}{2^{2l+1}}\frac{1}{l!}\left(\frac{i}{2\pi}\right)^l \int_{\mathcal{M}} \mathrm{tr}\left[Q(\mathrm{d}Q)^{2l}\right] = \frac{1}{l!}\left(\frac{i}{2\pi}\right)^l \int_{BZ^d} \mathrm{tr}\left(\mathcal{F}^l\right).$$

Here, $\mathcal{M}$ is the d-dimensional Brillouin zone and the Berry curvature

$$\mathcal{F} = \mathrm{d}\mathcal{A} + \mathcal{A}^2$$

is the $N \times N$-matrix form

$$\mathcal{F}^{mn} = \frac{1}{2}\left(\frac{\partial \mathcal{A}_{k_y}}{\partial k_x} - \frac{\partial \mathcal{A}_{k_x}}{\partial k_y} + \left[\mathcal{A}_{k_x}, \mathcal{A}_{k_y}\right]\right)^{mn} \mathrm{d}k_x \wedge \mathrm{d}k_y, \qquad 1 \le m, n \le N \qquad (d = 2)$$

defined in terms of the non-abelian Berry connection

$$\mathcal{A}^{mn} = \mathcal{A}^{mn}_{k_x}\mathrm{d}k_x + \mathcal{A}^{mn}_{k_y}\mathrm{d}k_y = \langle E_m|\,\partial_{k_x}\,|E_n\rangle\,\mathrm{d}k_x + \langle E_m|\,\partial_{k_y}\,|E_n\rangle\,\mathrm{d}k_y, \qquad 1 \le m, n \le N.$$

Example 9. Consider a two-band model

$$H(k) = d(k)\cdot\sigma := d_x(k)\sigma_x + d_y(k)\sigma_y + d_z(k)\sigma_z = \begin{pmatrix} d_z(k) & d_x(k) - id_y(k) \\ d_x(k) + id_y(k) & -d_z(k) \end{pmatrix},$$

with energies $E_\pm(k) = \pm|d(k)|$ and a Fermi energy $E_F = 0$. The Berry connection becomes

$$\mathcal{A} = \mathcal{A}_{k_x}\mathrm{d}k_x + \mathcal{A}_{k_y}\mathrm{d}k_y = \begin{pmatrix} \mathcal{A}^{++}_{k_x} & \mathcal{A}^{+-}_{k_x} \\ \mathcal{A}^{-+}_{k_x} & \mathcal{A}^{--}_{k_x} \end{pmatrix}\mathrm{d}k_x + \begin{pmatrix} \mathcal{A}^{++}_{k_y} & \mathcal{A}^{+-}_{k_y} \\ \mathcal{A}^{-+}_{k_y} & \mathcal{A}^{--}_{k_y} \end{pmatrix}\mathrm{d}k_y.$$

where $\mathcal{A}^{+-}_{k_x} = \langle E_+|\partial_{k_x}|E_-\rangle$ and the other components are defined analogously. The trace of the commutator $[\mathcal{A}_{k_x}, \mathcal{A}_{k_y}]$ vanishes and we are working in dimension $d = 2$, so the differential form to be integrated is

$$\mathrm{tr}(\mathcal{F}) = \mathcal{F}^{++} + \mathcal{F}^{--} = \frac{1}{2}\left(\frac{\partial \mathcal{A}^{++}_{k_y}}{\partial k_x} - \frac{\partial \mathcal{A}^{++}_{k_x}}{\partial k_y}\right)\mathrm{d}k_x \wedge \mathrm{d}k_y + \frac{1}{2}\left(\frac{\partial \mathcal{A}^{--}_{k_y}}{\partial k_x} - \frac{\partial \mathcal{A}^{--}_{k_x}}{\partial k_y}\right)\mathrm{d}k_x \wedge \mathrm{d}k_y.$$

It is sometimes useful to think of topological phases as homotopy classes of the ground state. Consider for example a deformation (homotopy) of one ground state U_0 into the ground state U_1 of another system[10], both with the same numbers $N_\pm$ of (un)occupied bands:

$$U_s(k) : [0,1] \times BZ \to U(N)/U(N_+) \times U(N_-).$$

The homotopy U_s is only well-defined if the numbers $N_\pm$ remain constant throughout the deformation, which is just another way of saying that the energy gap must remain open. If the two ground states cannot be continuously deformed into each other without closing the gap, then they belong to different homotopy classes and are therefore in different topological phases.

[10] Of course, what we are really deforming are the Q-matrices Q_0 and Q_1, not the ground states per se.

2.3.2 Symmetry classes

Multiparticle quantum systems are notoriously difficult to study and computational approaches quickly become unfeasible, as even microscopic systems can contain billions of particles and each particle adds more dimensions to the Hilbert space. A common way to significantly reduce the computational complexy involved is to use a so-called mean field approximation, in which the countless particle-particle interactions are replaced by a statistical *mean* interaction. Each particle can then be studied individually and the multiparticle system becomes a composition of non-interacting single-particle systems. Insight about electronic properties of a crystal, ignoring lattice dynamics, can thus be gained by studying the dynamics of a single electron.

Due to the stochastic nature of mean fields, Hamiltonians describing such non-interacting single-electron systems can be studied from the perspective of random matrix theory. Seminal work by Altland & Zirnbauer [2] has led to the complete classification of such matrices according to the presence or absence of three fundamental symmetries: *time-reversal invariance*, *particle-hole symmetry*, and *chiral symmetry*. We shall not go into detail about how these symmetries are normally defined, on the level of second quantization, as they can also be expressed in terms of operators acting on the first-quantized Hamiltonian that is more familiar to us. For example, chiral symmetry is characterized by the existence of a linear unitary operator Γ such that [25]

$$\Gamma H(t,k)\Gamma^\dagger = -H(-t,k).$$

Both time-reversal invariance (Θ) and particle-hole symmetry ($\mathcal{P}$) come in two flavours, determined by what happens when the same symmetry operator is applied twice: the different possibilities are $\Theta^2 = \pm\mathbb{1}$ and $\mathcal{P}^2 = \pm\mathbb{1}$. Chiral symmetry only comes in one flavour, $\Gamma^2 = +\mathbb{1}$, and can only exist either in the absence of other symmetries, or in the presence of both time-reversal invariance and particle-hole symmetry; presence of two symmetries implies presence of all three. Counting up the possibilities, we find that there are ten distinct combinations of symmetries with different flavours, and each combination defines one symmetry class.

An interesting property of topological insulators is that different symmetry classes and spatial dimensions correspond to different kinds of topological invariants, making it possible to classify such materials by their symmetries. Much work has gone into this classification, and has culminated in the periodic table of topological insulators shown in Table 2.1.

class$\backslash d$	Θ	$\mathcal{P}$	Γ	0	1	2	3	4	5	6	7
A	0	0	0	$\mathbb{Z}$	0	$\mathbb{Z}$	0	$\mathbb{Z}$	0	$\mathbb{Z}$	0
AIII	0	0	1	0	$\mathbb{Z}$	0	$\mathbb{Z}$	0	$\mathbb{Z}$	0	$\mathbb{Z}$
AI	+	0	0	$\mathbb{Z}$	0	0	0	$2\mathbb{Z}$	0	$\mathbb{Z}_2$	$\mathbb{Z}_2$
BDI	+	+	1	$\mathbb{Z}_2$	$\mathbb{Z}$	0	0	0	$2\mathbb{Z}$	0	$\mathbb{Z}_2$
D	0	+	0	$\mathbb{Z}_2$	$\mathbb{Z}_2$	$\mathbb{Z}$	0	0	0	$2\mathbb{Z}$	0
DIII	-	+	1	0	$\mathbb{Z}_2$	$\mathbb{Z}_2$	$\mathbb{Z}$	0	0	0	$2\mathbb{Z}$
AII	-	0	0	$2\mathbb{Z}$	0	$\mathbb{Z}_2$	$\mathbb{Z}_2$	$\mathbb{Z}$	0	0	0
CII	-	-	1	0	$2\mathbb{Z}$	0	$\mathbb{Z}_2$	$\mathbb{Z}_2$	$\mathbb{Z}$	0	0
C	0	-	0	0	0	$2\mathbb{Z}$	0	$\mathbb{Z}_2$	$\mathbb{Z}_2$	$\mathbb{Z}$	0
CI	+	-	1	0	0	0	$2\mathbb{Z}$	0	$\mathbb{Z}_2$	$\mathbb{Z}_2$	$\mathbb{Z}$

Table 2.1: Periodic table of topological insulators and superconductors; d denotes the spatial dimension and (A, AIII, ..., CI) denotes the ten Altland-Zirnbauer symmetry classes of fermionic Hamiltonians, which are characterized by the presence/absence of time-reversal (Θ), particle-hole ($\mathcal{P}$), and chiral (Γ) symmetry of different types denoted by ± 1. The entries "$\mathbb{Z}$", "$\mathbb{Z}_2$", and "0" represent the presence/absence of non-trivial gapped bulk topological insulators/superconductors, and when they exist, types of these states. (Table and caption taken from ref. [9].)

Example 10.

(a) The 2D quantum Hall effect corresponds to symmetry class A and is thus described by an integer topological invariant, namely the Chern number ν that determines the quantized Hall conductance. The quantum Hall effect has no analogue in odd dimensions.

(b) In the 2D quantum *spin* Hall effect, two spin-polarized currents flow in opposite directions along the boundary. This effect arises in 2D time-reversal invariant systems with $\Theta^2 = -\mathbb{1}$ (symmetry class AII) and is therefore described by a $\mathbb{Z}_2$ topological invariant, which has a physical interpretation as the number of helical edge modes (mod 2) [9].

3

Floquet Topological Superconductors

If topological behaviour can be induced in quantum systems through translational invariance and the nontrivial torus topology of the Brillouin zone, as was discussed in an earlier section, it makes sense to look for topological phenomena in systems with other types of invariance or periodicity. Especially interesting are *Floquet topological insulators*, which employ periodic driving to induce novel topological behaviour not found in more conventional static systems [21, 26], and which have been realized in acoustic [22], photonic [23], and solid state [35] systems. A homotopy-based classification scheme for Floquet topological insulators has been developed and applied to systems without symmetry [26] as well as to time-reversal invariant systems [8]. Our mission in this final chapter is to explain the classification scheme and to apply it to particle-hole symmetric systems. As a by-product, we achieve a classification of Floquet topological superconductors.

3.1 Floquet and quasienergy

Driving a system means actively interfering with the system in a manner that affects its energy levels over time, for example by applying a time-dependent magnetic field or by simply pumping in additional energy. The corresponding Hamiltonian can generally be written as the sum of a static, non-driven term and a time-dependent driving term:

$$H_{\text{full}}(t, k) = H_0(k) + H(t, k).$$

The driving is often described as either *weak* or *strong*, depending on how much it affects the overall dynamics: weak driving is used to analyse how a given system reacts to a small, time-dependent perturbation, whilst strong driving is more often used to control and direct the behaviour of a system. In both cases, one term in the Hamiltonian can be considered the main term and studied separately, after which the other term is added as a perturbation. To apply our results to real systems, one may therefore treat our general, time-periodic Hamiltonian either as the full Hamiltonian or specifically as the driving term in a strongly driven system.

We are interested in periodically driven systems, i.e. systems with a time-periodic Hamiltonian

$$H(t+T,k) = H(t,k)$$

with driving period T. Floquet theory, the branch of mathematics that deals with periodic linear systems of ordinary differential equations, can be applied to find the instantaneous eigenstates

$$|E_n(t,k)\rangle = e^{-i\epsilon_n(k)t}\,|u_n(t,k)\rangle\,, \qquad n = 1,\ldots,N,$$

where $|u_n(t,k)\rangle$ are time-periodic Floquet waves. Whenever the adiabatic theorem holds,

$$U(T,k)\,|E_n(t,k)\rangle = |E_n(t+T,k)\rangle = e^{-i\epsilon_n(k)(t+T)}\,|u_n(t+T,k)\rangle = e^{-i\epsilon_n(k)T}\,|E_n(t,k)\rangle\,,$$

so the instantaneous eigenstates are eigenstates of the *Floquet operator* $U(T,k)$. As it turns out, the concept of energy is ill-defined in driven systems so the time-dependent Hamiltonian is replaced by the Floquet operator that evolves time stroboscopically, one driving period at a time. The unitary Floquet operator is diagonalizable, so Kato's theorem implies the existence of bands

$$\lambda_n(k) = e^{-i\epsilon_n(k)T}$$

which are continuous and partially differentiable, and the same is true of the *quasienergy bands*

$$\epsilon_n(k) = -\frac{T}{2\pi}\phi^{-1}(\lambda_n(k)),$$

defined in terms of the diffeomorphism $\phi : \mathbb{R}/\mathbb{Z} \to \mathbb{T}$, $x \mapsto e^{2\pi i x}$. Quasienergies play a role analogous to that of ordinary energies in static systems and are defined mod $2\pi/T$.

The notation $\epsilon_n(k)$ will most often be used to denote real-valued representatives lying in the *quasienergy Brillouin zone* $(-\pi/T, \pi/T]$, just like the 2π-periodic crystal momenta k_x and k_y are almost always assumed to lie in the interval $(-\pi, \pi]$.

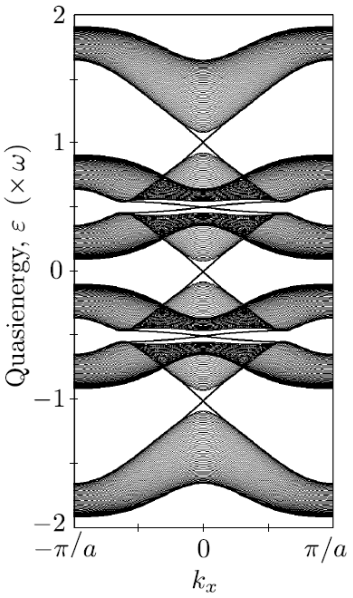

Figure 3.1: An example of a quasienergy band structure [26], which shares many similarities with energy band structures in static systems. Quasienergies are different from ordinary energies, however, in that they are defined mod $2\pi/T$. It is therefore possible for a quasienergy band to extend beyond the top of the band structure ($\epsilon = \pi/T$) and appear again at the bottom ($\epsilon = -\pi/T$). In this example, the quasienergies have been expressed in units of the driving frequency ω.

Example 11. If the Hamiltonian $H(t,k)$ is either time-independent or diagonal for each (t,k), one can define the time-evolution operator $U(t,k)$ without invoking the time-ordering operator $\mathcal{T}$. The corresponding Floquet operator $U(T,k)$ then simplifies to

$$U(T,k) = e^{-i\int_0^T H(s,k)\ \mathrm{d}s},$$

and the quasienergies $\epsilon_n(k)$ become the time-averaged energy content of the n'th energy band:

$$\epsilon_n(k) = \frac{1}{T}\int_0^T E_n(s,k)\ \mathrm{d}s,$$

of course taken mod $2\pi/T$. Such a concrete interpretation does not exist in general but, as we will see later on, the Floquet spectrum *does* provide physical information.

3.2 Particle-Hole Symmetry

Conduction in a crystal lattice is a manifestation of electrons being transported between different lattice sites. Each site can only support a finite number of electrons before it gets filled and conduction to that site stops, so it makes sense to think about the lattice sites as being occupied by a number of electrons and a complementary number of electron *holes*, representing the lack of an electron. Transportation of electrons in one direction is then equivalent to transportation of holes in the opposite direction, as illustrated in Figure 3.2.

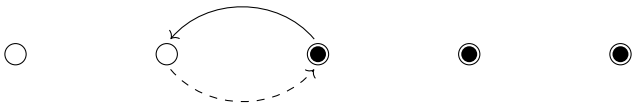

Figure 3.2: A negatively charged electron (filled circle) moving in one direction is equivalent to a positively charged electron hole moving in the opposite direction.

Switching the roles of electrons and holes in a quantum system $\mathcal{H}$ creates a new quantum system $\mathcal{H}'$, identical to the original system in every way except for the particle-hole role-reversal, and the two are related by an invertible *particle-hole operator* $\mathcal{P}:\mathcal{H}\to\mathcal{H}'$ mapping electron (hole) eigenstates in $\mathcal{H}$ to hole (electron) eigenstates in $\mathcal{H}'$:

$$H(t,k)\,|E_n\rangle = E_n\,|E_n\rangle \quad\Rightarrow\quad H'(t,-k)\mathcal{P}\,|E_n\rangle = -E_n\mathcal{P}\,|E_n\rangle\,, \tag{3.1}$$

where H (H') is the Hamiltonian associated with $\mathcal{H}$ ($\mathcal{H}'$). In a *particle-hole symmetric* system,

$$\mathcal{H} = \mathcal{H}' \qquad \text{and} \qquad H = H'.$$

Assuming $H = H'$ in Eq. (3.1), left-multiplication by $\langle E_m|\,\mathcal{P}^\dagger$ yields the relation

$$-E_m\,\langle E_m|\mathcal{P}^\dagger\mathcal{P}|E_n\rangle = \langle E_m|\mathcal{P}^\dagger H(t,-k)\mathcal{P}|E_n\rangle = -E_n\,\langle E_m|\mathcal{P}^\dagger\mathcal{P}|E_n\rangle\,,$$

which tells us that the particle-hole operator preserves the orthogonality relation between pairs of eigenstates $|E_m\rangle$ and $|E_n\rangle$ with different energy levels. If all of the energy levels are distinct, the states $\mathcal{P}\,|E_1\rangle\,,\ldots,\mathcal{P}\,|E_N\rangle$ form an orthonormal basis in $\mathcal{H}$ and we conclude that the particle-hole operator $\mathcal{P}$ is unitary. The beauty of this fact is that it holds for any time t and crystal moment k,

so the particle-hole operator is guaranteed to be unitary unless there are band crossings at every single point $(t, k) \in [0, T] \times BZ$, which would make for a highly erratic and physically unrealistic band structure. We thus assume, without loss of *significant* generality, that $\mathcal{P}$ is unitary.

Unfortunately, the particle-hole operator cannot be linear as that would break the underlying $U(1)$ gauge invariance of our electron system[1]. We still retain some degree of linearity, however, as the particle-hole operator is *anti*linear unitary - *antiunitary* for short.

Definition. An operator $\mathcal{P} : \mathcal{H} \to \mathcal{H}$ is said to be *antiunitary* if

$$\langle\phi|\mathcal{P}^\dagger\mathcal{P}|\varphi\rangle = \langle\varphi|\phi\rangle = \langle\phi|\varphi\rangle^*$$

for all $|\phi\rangle, |\psi\rangle \in \mathcal{H}$.

Readers unfamiliar with antilinear operators need not worry, as the following lemma shows that antilinear unitary operators have a very simple form: they are linear unitary operators multiplied by the complex conjugation operator $\mathcal{K}$ that conjugates coordinates. More precisely, any antiunitary operator can be written on the form $\mathcal{P} = \mathcal{P}\mathcal{K}^2 = P\mathcal{K}$, where $P = \mathcal{P}\mathcal{K}$ is linear unitary.

Lemma 1. *A linear operator P is unitary if and only if $\mathcal{P} = P\mathcal{K}$ is antiunitary.*

Proof. Let $|\psi_1\rangle, |\psi_2\rangle, |\psi_3\rangle, \ldots$ be an orthonormal basis in $\mathcal{H}$ and expand $|\phi\rangle, |\varphi\rangle \in \mathcal{H}$ as

$$|\phi\rangle = \sum_n \langle\psi_n|\phi\rangle |\psi_n\rangle, \qquad |\varphi\rangle = \sum_n \langle\psi_n|\varphi\rangle |\psi_n\rangle.$$

The defining property of the complex conjugation operator is that it conjugates coordinates,

$$|\psi^*\rangle := \mathcal{K}|\psi\rangle = |\psi\rangle^* = \left(\sum_n \langle\psi_n|\psi\rangle |\psi_n\rangle\right)^* = \sum_n \langle\psi_n|\psi\rangle^* |\psi_n\rangle = \sum_n \langle\psi|\psi_n\rangle |\psi_n\rangle,$$

so if P is unitary, then

$$\langle\phi|\mathcal{K}^\dagger P^\dagger P\mathcal{K}|\varphi\rangle = \langle\phi^*|P^\dagger P|\varphi^*\rangle = \langle\phi^*|\varphi^*\rangle = \sum_n \langle\varphi|\psi_n\rangle\langle\psi_n|\phi\rangle = \langle\varphi|\mathbb{1}|\phi\rangle = \langle\varphi|\phi\rangle,$$

which means that $\mathcal{P} = P\mathcal{K}$ is antiunitary. The proof of the other direction is analogous. □

By unitarity and Eq. (3.1),

$$\langle E_m|H(t,k)|E_n\rangle = E_n\delta_{mn} = E_n\langle E_m|\mathcal{P}^\dagger\mathcal{P}|E_n\rangle = -\langle E_m|\mathcal{P}^\dagger H(t,-k)\mathcal{P}|E_n\rangle,$$

so the operators $H(t, k)$ and $-\mathcal{P}^\dagger H(t, -k)\mathcal{P}$ have the same eigenkets and the same eigenvalues, and are therefore equal.

Definition. A system is said to have *particle-hole symmetry* (PHS) if there exists an antiunitary *particle-hole operator* $\mathcal{P} = P\mathcal{K}$ acting on the Hamiltonian by

$$\mathcal{P}H(t,k)\mathcal{P}^\dagger = -H(t,-k),$$

for all (t, k).

[1] In the language of second quantization, the particle-hole operator switches the roles of creation and annihilation operators: $\mathcal{P}c_k^\dagger\mathcal{P}^\dagger = c_{-k}$. Antilinear operators conjugate complex phases, $\mathcal{P}e^{i\theta}\mathcal{P}^{-1} = e^{-i\theta}$, and thereby preserve the underlying invariance under $U(1)$ gauge transformations $c_k^\dagger \mapsto e^{i\theta}c_k^\dagger$.

The energy band structure of a PHS Hamiltonian is odd in crystal momentum, as implied by Eq. (3.1), but we cannot say the same about the individual energy bands. This is because the particle-hole operator need not preserve band indices.

Example 12. The toy Hamiltonian

$$H(k) = \begin{pmatrix} \sin(k) & i\cos(k) \\ -i\cos(k) & \sin(k) \end{pmatrix}, \qquad (k = k_x)$$

has PHS under $\mathcal{P} = \sigma_x \mathcal{K}$, and smooth energy bands $E_\pm(k) = \sin(k) \pm \cos(k)$. The band structure is evidently odd in crystal momentum (Figure 3.3) but the individual energy bands are not.

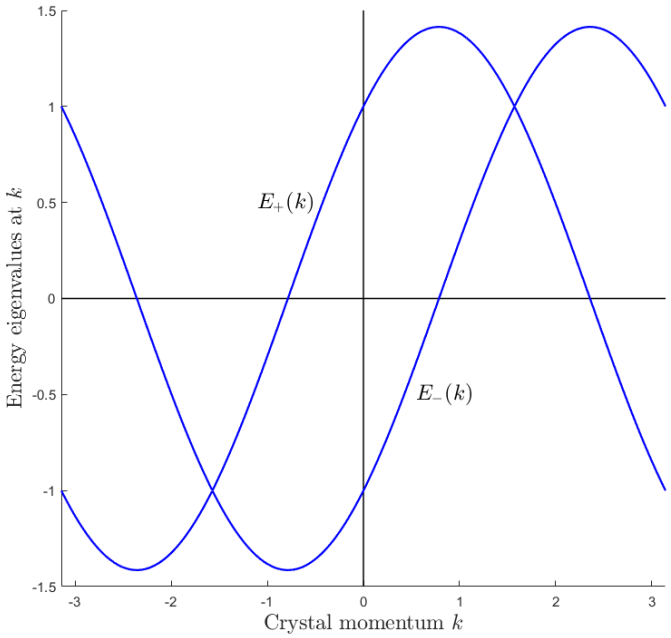

Figure 3.3: The band structure of a PHS Hamiltonian $H(k)$ is odd in k.

3.2.1 Relation to superconductivity

We touched upon second quantization in the previous chapter but only very briefly, so let us give a more detailed introduction before explaining the relation between particle-hole symmetry and superconductivity. First recall the existence of *creation* and *annihilation operators* $c^\dagger_{nk}$ and c_{nk} which act on a multiparticle state $|\psi\rangle$ to create or annihilate an electron at crystal momentum k and energy $\mathcal{E}_n(k)$. It is impossible for more than one electron to occupy the same energy state, due to the Pauli exclusion principle, and any attempt to create an electron at an already occupied energy has the effect of killing the state ($c^\dagger_{nk}|\psi\rangle = 0$). The same is true if one attempts to annihilate an electron at an already unoccupied energy ($c_{nk}|\psi\rangle = 0$). The following operator can therefore be used to check the occupation of the corresponding energy level:

$$c^\dagger_{nk} c_{nk} |\psi\rangle = \begin{cases} |\psi\rangle\ , & \text{if the energy level } \mathcal{E}_n(k) \text{ is occupied,} \\ 0\ , & \text{if the energy level } \mathcal{E}_n(k) \text{ is unoccupied,} \end{cases}$$

and by extension, the number operator $\hat{N} := \sum_{n,k} c_{nk}^\dagger c_{nk}$ determines the total occupation number:

$$\hat{N}\,|\psi\rangle = \sum_{n,k} c_{nk}^\dagger c_{nk}\,|\psi\rangle = \left(\sum_{\substack{\text{occupied}\\ \text{levels}}} 1\right)|\psi\rangle\,.$$

The probability distribution of the number operator $\hat{N}$ tends to have a sharp peak around $\langle\hat{N}\rangle$, which tells us that the total number of electrons in a typical quantum system is more or less fixed.

Excitations, collisions, and similar kinds of processes are represented by operators $c_{ml}^\dagger c_{nk}$ which annihilates an electron in one energy state and creates an electron in another energy state, and one can prove that fermionic creation and annihilation operators satisfy the anti-commutation relations

$$\left\{c_{ml}, c_{nk}^\dagger\right\} = \delta_{mn}\delta_{lk}, \qquad \text{and} \qquad \left\{c_{ml}, c_{nk}\right\} = \left\{c_{ml}^\dagger, c_{nk}^\dagger\right\} = 0.$$

The unoccupied *vacuum* state $|0\rangle$ is defined as an eigenvector $\hat{N}\,|0\rangle = 0$ of the number operator, and the quantum ground state is constructed by filling every energy level up to the Fermi energy:

$$|gs\rangle := \prod_{\mathcal{E}_n(k)\le\mathcal{E}_F} c_{nk}^\dagger\,|0\rangle\,.$$

Let us now look at how superconductors are described in second quantization, following section III. of ref. [28]. In the absence of spin[2], a superconducting single-band Hamiltonian can be written as[3]

$$\mathcal{H} = \sum_k \mathcal{E}(k) c_k^\dagger c_k + \frac{1}{2}\sum_{k,l} V(k,l) c_k^\dagger c_{-k}^\dagger c_{-l} c_l,$$

where $V(k,l)$ is a pairing interaction between electrons with crystal momentum k, l, and the operators $c_{-k}^\dagger c_k^\dagger$ and $c_{-l}c_l$ respectively represent creation and annihilation of a Cooper pair. Rather than studying this Hamiltonian directly, we make an approximation [33]

$$c_k^\dagger c_{-k}^\dagger c_{-l} c_l \approx c_k^\dagger c_{-k}^\dagger \langle c_{-l} c_l\rangle + \langle c_k^\dagger c_{-k}^\dagger\rangle c_{-l} c_l$$

and observe that $\langle c_k^\dagger c_{-k}^\dagger\rangle = \langle c_{-k} c_k\rangle^*$. If we now define a pair interaction $\Delta(k) = \sum_l V(k,l)\,\langle c_{-l} c_l\rangle$, we obtain an approximate Hamiltonian that is free from interactions between different Cooper pairs:

$$\mathcal{H} \approx \sum_k \mathcal{E}(k) c_k^\dagger c_k + \frac{1}{2}\sum_k \Big(\Delta(k) c_k^\dagger c_{-k}^\dagger + \Delta(k)^* c_{-k} c_k\Big). \tag{3.2}$$

Note that the above Hamiltonian allows for individual Cooper pairs to be added to or removed from the system, so a superconductor does not have a fixed occupation number $\langle\hat{N}\rangle$.

The above Hamiltonian can be rewritten on the more succinct *Bogoliubov-de-Gennes* form

$$\mathcal{H} \approx \frac{1}{2}\sum_k \psi_k^\dagger H_{\mathrm{BdG}}(k)\psi_k + \frac{1}{2}\sum_k \mathcal{E}(k), \tag{3.3}$$

where

$$\psi_k = \begin{pmatrix} c_k \\ c_{-k}^\dagger \end{pmatrix}, \qquad \text{and} \qquad H_{\mathrm{BdG}}(k) = \begin{pmatrix} \mathcal{E}(k) & \Delta(k) \\ \Delta(k)^* & -\mathcal{E}(-k) \end{pmatrix}.$$

[2]Spin is an intrinsic form of angular momentum that we ignore partly for simplicity, partly because we are mainly interested in topological p-wave superconductors where both electrons in a Cooper pair have the same spin.

[3]The sum exists because the number of crystal momenta is strictly speaking finite. Our use of a continuous Brillouin zone $BZ \simeq \mathbb{T}^2$ is a well-established simplification within condensed matter physics that has proven to work in practice. Also, the single band index $n = 1$ is superfluous and has been dropped.

The easiest way to show this relation is to start with the right-hand side of Eq. (3.3) and prove that it equals the right-hand side of Eq. (3.2). Ordinary matrix multiplication yields the expression

$$\psi_k^\dagger H_{\text{BdG}}(k)\psi_k = \mathcal{E}(k)c_k^\dagger c_k + \Delta(k)c_k^\dagger c_{-k}^\dagger + \Delta(k)^* c_{-k}c_k - \mathcal{E}(-k)c_{-k}c_{-k}^\dagger$$

for any fixed value of k, hence the sum over k can be rewritten in the following way:

$$\begin{aligned}\frac{1}{2}\sum_k \psi_k^\dagger H_{\text{BdG}}(k)\psi_k &= \frac{1}{2}\sum_k \Big(\mathcal{E}(k)c_k^\dagger c_k + \Delta(k)c_k^\dagger c_{-k}^\dagger + \Delta(k)^* c_{-k}c_k - \mathcal{E}(-k)c_{-k}c_{-k}^\dagger\Big) = \\ &= \frac{1}{2}\sum_k \Big(\mathcal{E}(k)\big(c_k^\dagger c_k - c_k c_k^\dagger\big) + \Delta(k)c_k^\dagger c_{-k}^\dagger + \Delta(k)^* c_{-k}c_k\Big).\end{aligned}$$

The anti-commutation relation $\{c_k, c_l^\dagger\} = \delta_{kl}$ implies that $c_k^\dagger c_k - c_k c_k^\dagger = 2c_k^\dagger c_k - 1$, so

$$\begin{aligned}\frac{1}{2}\sum_k \psi_k^\dagger H_{\text{BdG}}(k)\psi_k &= \frac{1}{2}\sum_k \Big(\mathcal{E}(k)\big(2c_k^\dagger c_k - 1\big) + \Delta(k)c_k^\dagger c_{-k}^\dagger + \Delta(k)^* c_{-k}c_k\Big) = \\ &= \sum_k \mathcal{E}(k)c_k^\dagger c_k + \frac{1}{2}\sum_k \Big(\Delta(k)c_k^\dagger c_{-k}^\dagger + \Delta(k)^* c_{-k}c_k\Big) - \frac{1}{2}\sum_k \mathcal{E}(k),\end{aligned}$$

which is precisely what we set out to prove. The constant term $\frac{1}{2}\sum_k \mathcal{E}(k)$ does not contribute to the overall dynamics and can therefore be dropped, so the full Hamiltonian $\mathcal{H}$ is approximated as

$$\mathcal{H} \approx \frac{1}{2}\sum_k \psi_k^\dagger H_{\text{BdG}}(k)\psi_k,$$

and we observe that the BdG Hamiltonian is particle-hole symmetric under $\mathcal{P} = \sigma_x\mathcal{K}$:

$$\mathcal{P}H_{\text{BdG}}(k)\mathcal{P}^{-1} = -\mathcal{H}_{\text{BdG}}(-k).$$

Furthermore, applying a Bogoliubov transformation [28] puts the above Hamiltonian on the form

$$\mathcal{H} \approx \sum_{n=1}^{2}\sum_k E_n(k)\alpha_{nk}^\dagger\alpha_{nk},$$

where $E_n(k)$ are the eigenvalues of the BdG Hamiltonian and $\alpha_{nk}^\dagger, \alpha_{nk}$ satisfy the definition of fermionic creation and annihilation operators. The Hamiltonian $\mathcal{H}$ thus approximates a system of non-interacting *Bogoliubov quasiparticles*, each described by the single-particle Hamiltonian H_{BdG}.

The story is much the same in a superconducting system with $n = 1, \ldots, N$ bands $\mathcal{E}_n$. Higher-dimensional analogues of the calculations performed above show [28] that $\mathcal{H}$ approximates a system of non-interacting fermionic quasiparticles, each of which is described by a BdG Hamiltonian of dimension $2N \times 2N$. In other words, superconductors have the same type of band structure as particle-hole symmetric single-particle Hamiltonians and will therefore be covered by our analysis.

3.3 Probing the quasienergy gap

It is finally time to describe the classification scheme developed by Rudner and colleagues [26], starting with a system with trivial Floquet operator $U(T, k) = \mathbb{1}$. The corresponding time-evolution operator is periodic not only in crystal momentum, but also in time,

$$U(t + T, k) = U(t, k)U(T, k) = U(t, k).$$

and thereby defines a continuous map $U : \mathbb{T}^3 \to U(N)$. Recall that the torus $\mathbb{T}^3 = S^1 \times S^1 \times S^1$ simply consists of three copies of the unit circle so by setting two of the three parameters t, k_x, k_y to 0, the time-evolution operator becomes a continuous loop $S^1 \to U(N)$ based at $U(0,0) = \mathbb{1}$ and thus represents a homotopy class in the fundamental group $\pi_1(U(N)) \simeq \mathbb{Z}$. This immediately implies the existence of three integer topological invariants - specifically three winding numbers [8]

$$w_{\mathcal{C}_i}[U] = \frac{1}{2\pi i} \int_{\mathcal{C}_i} \mathrm{d} \log \det U, \qquad i = t, k_x, k_y,$$

one for each of the three loops

$$\mathcal{C}_t = S^1 \times \{0\} \times \{0\}, \qquad \mathcal{C}_{k_x} = \{0\} \times S^1 \times \{0\}, \qquad \mathcal{C}_{k_y} = \{0\} \times \{0\} \times S^1, \tag{3.4}$$

with the obvious orientations. Two of these winding numbers vanish for any Floquet system since[4]

$$w_{\mathcal{C}_i}[U] = \frac{1}{2\pi i} \int_{-\pi}^{\pi} \frac{\partial_i \det U(0,i)}{\det U(0,i)} \, \mathrm{d}i = \big[U(0,i) = \mathbb{1}\big] = 0, \qquad i = k_x, k_y,$$

but the third one, $w_{\mathcal{C}_t}[U]$, does not vanish in general. We refer to it simply as *the winding number* and though it does not have a natural physical interpretation, it is interesting for purely mathematical reasons. The winding number will be studied in greater detail in Section 4.4.

A natural next step in the search for (additional) topological invariants is to look at higher homotopy groups π_d of the unitary group $U(N)$. The second homotopy group is trivial, however, and the dimension of our parameter manifold $\mathbb{T}^3$ prevents us from relating the time-evolution to any homotopy group higher than π_3. Fortunately, there is a $\pi_3 \simeq \mathbb{Z}$ topological invariant that is not only useful for classification purposes, but which also has an important physical interpretation.

The elements of $\pi_3(U(N))$ are homotopy classes of continuous maps $S^3 \to U(N)$, so the idea is to construct a quotient $q : \mathbb{T}^3 \to S^3$ and then find a continuous map $\tilde{U} : S^3 \to U(N)$ that is unique up to homotopy and satisfies $U = \tilde{U} \circ q$, as per the following commutative diagram.

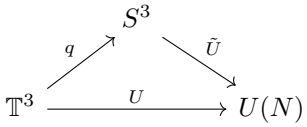

The process is best illustrated by stepping down to a lower dimension: a common way of constructing the 2-torus is to take the unit square $I = [0,1] \times [0,1]$ and identify opposite edges with each other, by means of the quotient map

$$q(x,y) = \begin{cases} (x,y)\ , & 0 < x < 1 \text{ and } 0 < y < 1, \\ (0,y)\ , & x \in \{0,1\} \text{ and } 0 < y < 1, \\ (x,0)\ , & 0 < x < 1 \text{ and } y \in \{0,1\}, \\ (0,0)\ , & x \in \{0,1\} \text{ and } y \in \{0,1\}. \end{cases}$$

We have illustrated the quotient $q(I) \simeq \mathbb{T}^2$ in Figure 3.4a. The curves

$$\mathcal{C}_1, \mathcal{C}_2 : [0,1] \to \mathbb{T}^2$$

defined by $\mathcal{C}_1(x) = (x,0)$ and $\mathcal{C}_2(y) = (0,y)$ can then be composed to a loop $\mathcal{C}_1\mathcal{C}_2\mathcal{C}_1^{-1}\mathcal{C}_2^{-1}$ around the "boundary" in Figure 3.4a and if we collapse this loop to a point, the torus becomes a sphere.

[4]The notation $(0,i)$ is short-hand for $(0,i,0)$ and $(0,0,i)$, depending on whether $i = k_x$ or $i = k_y$.

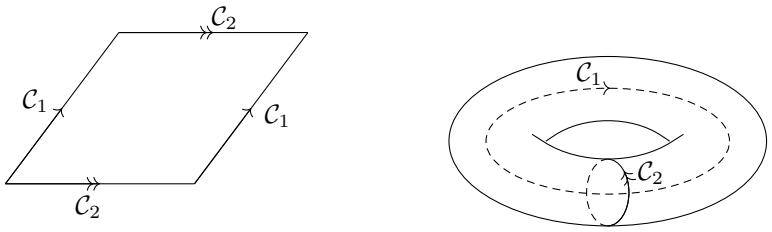

(a) **(b)**

Figure 3.4: One way to construct the 2-torus is to glue together opposite edges on a square. The loop $\mathcal{C}_1\mathcal{C}_2\mathcal{C}_1^{-1}\mathcal{C}_2^{-1}$ then traces around the edge and if we collapse it to a point, we get the 2-sphere.

The story is much the same in three dimensions: the 3-torus can be constructed from the unit cube and the three loops $\mathcal{C}_t, \mathcal{C}_{k_x}, \mathcal{C}_{k_y}$ defined in Eq. (3.4) are composed into a loop

$$\mathcal{L} = \mathcal{C}_t\mathcal{C}_{k_x}\mathcal{C}_{k_y}\mathcal{C}_t^{-1}\mathcal{C}_{k_x}^{-1}\mathcal{C}_{k_y}^{-1},$$

which is then collapsed to form the 3-sphere [8], using the quotient map

$$q(x) = \begin{cases} 0, & x \in \mathcal{L} \\ x, & x \notin \mathcal{L} \end{cases}$$

We view the elements $q(x)$ as equivalence classes $[x]$, which makes for cleaner notation.

Lemma 2. *The quotient map $q : \mathbb{T}^3 \to S^3$ is closed.*

Proof. For any closed set $V \subset \mathbb{T}^3$, the preimage

$$q^{-1}\big(q(V)\big) = \begin{cases} V\,, & 0 \notin V \\ V \cup \mathcal{L}\,, & 0 \in V \end{cases}$$

is also closed in $\mathbb{T}^3$, so the definition of quotient topology immediately implies that the image $q(V)$ is closed in S^3. In other words, q maps closed sets to closed sets. □

The time-evolution operator U is homotopic to a map that is constant on $\mathcal{L}$ [8] and we are only interested in homotopy-invariant behaviour, so we may assume without loss of generality that U is constant on $\mathcal{L}$. The map $\tilde{U}$ we talked about above is then defined as

$$\begin{aligned} \tilde{U} : S^3 &\to U(N) \\ [x] &\mapsto U(x) \end{aligned}$$

Lemma 3. *The map $\tilde{U}$ is continuous.*

Proof. First note that $\tilde{U}$ is well-defined, because the only equivalence class $[x]$ with more than one member is $[0] = q(\mathcal{L})$, and we have already assumed that U is constant on $\mathcal{L}$.

For any set $V \subset \mathbb{T}^3$, the inverse images of U and $\tilde{U}$ are related by

$$\tilde{U}^{-1}(V) = q\big(U^{-1}(V)\big)$$

and the continuity of U means that $U^{-1}(V)$ is closed in $\mathbb{T}^3$ whenever V is closed in $U(N)$. The lemma now follows from the fact that q is a closed map. □

The map $\tilde{U} : S^3 \to U(N)$ is a representative of some homotopy class in $\pi_3(U(N)) \simeq \mathbb{Z}$ and provides us with our last and most important topological invariant [17]

$$\deg(U) := \frac{1}{8\pi^2} \int_{\mathbb{T}^3} \mathrm{tr}\left(U^\dagger \partial_t U \left[U^\dagger \partial_{k_x} U, U^\dagger \partial_{k_y} U\right]\right) \mathrm{d}k_x \wedge \mathrm{d}k_y \wedge \mathrm{d}t, \tag{3.5}$$

which we call the *degree* of the time-evolution [8].

Now that we have established the existence of two topological invariants, namely the winding number and the degree, we must answer an important question: where is the physics in all of this? Is there an observable difference between two topologically distinct time-evolution operators? The answer is *yes*. In a system with trivial Floquet operator $U(T,k) = \mathbb{1}$, which has a single, large quasienergy gap at $\epsilon = \pi/T$, the degree counts the number of chiral edge states inside the gap [26]:

$$\deg(U) = n_{\mathrm{edge}}(\pi/T).$$

A system with non-trivial Floquet operator does not have a time-periodic time-evolution operator, so we can construct neither winding number nor degree. In fact, even if the degree could be computed, we would not know how to interpret it in terms of chiral edge states since the Floquet spectrum may contain more than one quasienergy gap. Both of these problems can be solved by constructing a family of quasienergy gap-dependent auxiliary operators [8, 26]

$$V_\epsilon : \mathbb{T}^3 \to U(N),$$

such that V_ϵ is homotopic to the time-evolution operator of a system with trivial Floquet operator. Both the winding number and the degree are then well-defined topological invariants and the degree can be interpreted as the number of chiral edge states in the gap at ϵ:

$$\deg(V_\epsilon) = n_{\mathrm{edge}}(\epsilon).$$

3.3.1 Construction of V_ϵ

The idea is to construct a gap-dependent effective Hamiltonian $H_\epsilon^{\mathrm{eff}}(k)$ that acts as a logarithm of the Floquet operator $U(T,k) = e^{-iTH_\epsilon^{\mathrm{eff}}(k)}$, and then define V_ϵ as the product

$$V_\epsilon(t,k) = U(t,k) e^{itH_\epsilon^{\mathrm{eff}}(k)}.$$

To construct the effective Hamiltonian, let $\lambda_n(k) = e^{-i\epsilon_n(k)T}$ denote the eigenvalues of the Floquet operator, with corresponding eigenkets $|\psi_n(k)\rangle$. Suppose $\epsilon \in \mathbb{R}$ lies in a quasienergy gap, meaning that $e^{-i\epsilon T} \neq e^{-i\epsilon_n(k)T}$ for every band n and each crystal momentum k, and let ϵ define a branch of the complex logarithm:

$$\ln_\epsilon\left(e^{-i\varphi T}\right) = -i\varphi T, \qquad \epsilon < \varphi < \epsilon + \frac{2\pi}{T}.$$

We then define the gap-dependent effective Hamiltonian as the Hermitian operator

$$H_\epsilon^{\mathrm{eff}}(k) := \frac{i}{T} \sum_{n=1}^{N} \ln_\epsilon\left(\lambda_n(k)\right) |\psi_n(k)\rangle \langle\psi_n(k)|.$$

The complex logarithm picks out a representative of each quasienergy $\epsilon_n(k)$ in a manner that depends on the choice of complex branch - or, equivalently, on the choice of quasienergy gap. Note that ϵ and ϵ' define the same effective Hamiltonian if and only if they lie in the same gap:

$$H_\epsilon^{\mathrm{eff}}(k) = H_{\epsilon'}^{\mathrm{eff}}(k) \quad \Longleftrightarrow \quad \ln_\epsilon\left(\lambda_n(k)\right) = \ln_{\epsilon'}\left(\lambda_n(k)\right) \text{ for } n = 1, \ldots, N.$$

One may easily confirm that the effective Hamiltonian exponentiates to the Floquet operator:

$$U(T,k) = e^{-iTH_\epsilon^{\text{eff}}(k)},$$

so the effective Hamiltonian satisfies the desired criteria.

Lemma 4. *The operator V_ϵ is unitary and time-periodic.*

Proof. Unitarity follows because $U(t,k)$ is unitary and $H_\epsilon^{\text{eff}}(k)$ is Hermitian:

$$V_\epsilon^\dagger(t,k)V_\epsilon(t,k) = \left(e^{-itH_\epsilon^{\text{eff}}(k)}U^\dagger(t,k)\right)\left(U(t,k)e^{itH_\epsilon^{\text{eff}}(k)}\right) = e^{-itH_\epsilon^{\text{eff}}(k)}e^{itH_\epsilon^{\text{eff}}(k)} = \mathbb{1},$$

and time-periodicity is equally straightforward:

$$V_\epsilon(t+T,k) = U(t+T,k)e^{i(t+T)H_\epsilon^{\text{eff}}(k)} = U(t,k)\underbrace{U(T,k)e^{iTH_\epsilon^{\text{eff}}(k)}}_{\mathbb{1}}e^{itH_\epsilon^{\text{eff}}(k)} = V_\epsilon(t,k).$$

□

Lemma 5. *If the projections $P_n(k) = |\psi_n(k)\rangle\langle\psi_n(k)|$ are continuous in k, then V_ϵ is continuous.*

Proof. The time-evolution operator is continuous in time and so is the exponential $e^{itH_\epsilon^{\text{eff}}(k)}$,

$$\|e^{i(t+\delta t)H_\epsilon^{\text{eff}}(k)} - e^{itH_\epsilon^{\text{eff}}(k)}\| \leq \|e^{itH_\epsilon^{\text{eff}}(k)}\|\|e^{i\delta tH_\epsilon^{\text{eff}}(k)} - \mathbb{1}\| \to 0, \qquad \delta t \to 0.$$

The same is therefore true of the product $V_\epsilon(t,k) = U(t,k)e^{itH_\epsilon^{\text{eff}}(k)}$.

Continuity in crystal momentum is more subtle. Since the quasienergy gap ϵ must lie in-between different bands λ_n, any pair of points in the *same* band must lie on the same side of the branch cut, so the quasienergy representatives $\epsilon_n(k) := \frac{i}{T}\ln_\epsilon\left(\lambda_n(k)\right)$ are continuous functions $BZ \to \mathbb{R}$. Assuming that the projectors $P_n(k)$ are continuous, we obtain the estimate

$$\|H_\epsilon^{\text{eff}}(k+\delta k) - H_\epsilon^{\text{eff}}(k)\| = \left\|\sum_n\left(\epsilon_n(k+\delta k)P_n(k+\delta k) - \epsilon_n(k)P_n(k)\right)\right\| \leq$$
$$\leq \sum_n |\epsilon_n(k+\delta k) - \epsilon_n(k)|\|P_n(k)\| + \sum_n |\epsilon_n(k+\delta k)|\,\|P_n(k+\delta k) - P_n(k)\|$$

which vanishes in the limit $\delta k \to 0$, proving that the effective Hamiltonian is continuous in crystal momentum; the same is then true of the exponential $e^{itH_\epsilon^{\text{eff}}(k)}$ and, by extension, V_ϵ. □

Remark 3. It is stated without proof in ref. [8] that the effective Hamiltonian becomes smooth whenever $H(t,k)$ is smooth, but we have been unable to rigorously prove this result or to back it up by independent sources. On the other hand, the projections originate from the Floquet operator

$$U(T,k) = \sum_n \lambda_n(k)\,|\psi_n(k)\rangle\langle\psi_n(k)| = \sum_n \lambda_n(k)P_n(k)$$

which is known to inherit smoothness from the Hamiltonian $H(t,k)$ and this may very well be enough to prove that V_ϵ is continuous. It would have been interesting to look further into the matter, given more time. The above Lemma can be considered a partial result and the rest of our analysis shall be conducted under the assumption that V_ϵ is continuous.

Even though the integral expression (3.5) for the degree contains partial derivatives, we only need continuity for $\deg V_\epsilon$ to be well-defined. This is because any continuous map $\mathbb{T}^3 \to U(N)$ is homotopy-equivalent to a smooth map, by the Whitney Approximation Theorem [20], and the degree can be calculated using this smooth representative.

3.3.2 Mirror-symmetry in the spectrum

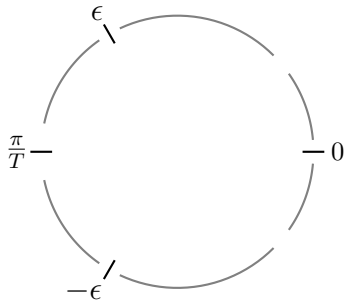

Figure 3.5: The mirror-symmetric gapped Floquet spectrum of a PHS Hamiltonian.

Everything we have done thus far is known, we have not done anything new, so let us change that by examining the effect that particle-hole symmetry has on our theory. The following proposition tells us that interchanging particles and holes does not have any particular effect on the time-evolution, other than reversing crystal momentum.

Proposition 6. *Suppose that the Hamiltonian $H(t,k)$ has particle-hole symmetry under $\mathcal{P} = P\mathcal{K}$. Then the time-evolution operator $U(t,k)$ satisfies*

$$\mathcal{P}U(t,k)\mathcal{P}^{-1} = U(t,-k).$$

Proof. Consider the partial sum

$$S_N(t,k) = \mathbb{1} + \sum_{n=1}^{N}(-i)^n \int_0^t \int_0^{t_1} \cdots \int_0^{t_{n-1}} H(t_1,k)\cdots H(t_n,k)\ \mathrm{d}t_1 \cdots \mathrm{d}t_n$$

and recall that $\lim_{N\to\infty} S_N(t,k) = U(t,k)$. The anti-unitary operator $\mathcal{P}$ flips the sign of the imaginary unit i and commutes with integration, so it follows that

$$\begin{aligned}\mathcal{P}S_N(t,k)\mathcal{P}^{-1} &= \mathbb{1} + \sum_{n=1}^{N}(+i)^n \int_0^t \int_0^{t_1} \cdots \int_0^{t_{n-1}} \underbrace{\mathcal{P}H(t_1,k)\mathcal{P}^{-1}}_{-H(t_1,-k)} \cdots \underbrace{\mathcal{P}H(t_n,k)\mathcal{P}^{-1}}_{-H(t_n,-k)}\ \mathrm{d}t_1 \cdots \mathrm{d}t_n = \\ &= \mathbb{1} + \sum_{n=1}^{N}(-i)^n \int_0^t \int_0^{t_1} \cdots \int_0^{t_{n-1}} H(t_1,-k)\cdots H(t_n,-k)\ \mathrm{d}t_1 \cdots \mathrm{d}t_n = S_N(t,-k).\end{aligned}$$

Letting $N \to \infty$ concludes the proof. □

Lemma 6. *The quasienergy band structure of a particle-hole symmetric system is mirror-symmetric under $\epsilon \mapsto -\epsilon$ (cf. Figure 3.5). Furthermore, the effective Hamiltonian transforms like*

$$\mathcal{P}H^{\mathit{eff}}_{\epsilon}(k)\mathcal{P}^{-1} = -H^{\mathit{eff}}_{-\epsilon-2\pi/T}(-k).$$

under the particle-hole operator $\mathcal{P}$.

Proof. Let $|\psi_n(k)\rangle$ denote the n'th eigenstate of the Floquet operator $U(T,k)$, with corresponding eigenvalue $\lambda_n(k) = e^{-i\epsilon_n(k)T}$. As the Floquet operators at k and $-k$ are related by particle-hole symmetry, $\mathcal{P}U(T,k)\mathcal{P}^{-1} = U(T,-k)$, we can extract the spectrum at $-k$ from the spectrum at k:

$$U(T,-k)\mathcal{P}\,|\psi_n(k)\rangle = \mathcal{P}U(T,k)\,|\psi_n(k)\rangle = \mathcal{P}\lambda_n(k)\,|\psi_n(k)\rangle = \lambda_n(k)^*\mathcal{P}\,|\psi_n(k)\rangle\,,$$

so the eigenstates of $U(T,-k)$ are on the form

$$|\psi_m(-k)\rangle = \mathcal{P}\,|\psi_n(k)\rangle\,, \tag{3.6}$$

with eigenvalues

$$e^{-i\epsilon_m(-k)T} = \lambda_m(-k) = \lambda_n(k)^* = e^{i\epsilon_n(k)T}.$$

The quasienergy band structure is therefore mirror-symmetric, proving our first claim. A direct consequence of this result is that the existence of a gap at ϵ implies the existence of a gap at $-\epsilon$.

Now choose a branch point $\epsilon \in \mathbb{R}$, assumed to lie inside a quasienergy gap, and let

$$\epsilon_n(k) := \frac{i}{T}\ln_\epsilon\big(\lambda_n(k)\big), \qquad n = 1,\dots,N,$$

be real-valued representatives of the quasienergies at k. By definition, these representatives satisfy

$$\epsilon < \epsilon_n(k) < \epsilon + \frac{2\pi}{T} \qquad \Longleftrightarrow \qquad -\epsilon - \frac{2\pi}{T} < -\epsilon_n(k) < -\epsilon,$$

so we can force the relation[5]

$$\epsilon_m(-k) = -\epsilon_n(k)$$

by defining the representatives $\epsilon_m(-k)$ at crystal momentum $-k$ using the branch point $-\epsilon - \frac{2\pi}{T}$:

$$\epsilon_m(-k) := \ln_{-\epsilon-2\pi/T}\big(\lambda_m(-k)\big), \qquad m = 1,\dots,N.$$

This branch point corresponds to the same position on the unit circle as $-\epsilon$, and is therefore guaranteed to lie inside a quasienergy gap. Our second claim now follows from a short calculation:

$$\begin{aligned}
H^{\text{eff}}_{-\epsilon-2\pi/T}(-k) &:= \frac{i}{T}\sum_{m=1}^{N}\ln_{-\epsilon-2\pi/T}\big(\lambda_m(-k)\big)\,|\psi_m(-k)\rangle\,\langle\psi_m(-k)| = \\
&= \sum_{m=1}^{N}\epsilon_m(-k)\,|\psi_m(-k)\rangle\,\langle\psi_m(-k)| = \\
&= \sum_{n=1}^{N}-\epsilon_n(k)\mathcal{P}\,|\psi_n(k)\rangle\,\langle\psi_n(k)|\,\mathcal{P}^{-1} = \\
&= -\mathcal{P}\left(\sum_{n=1}^{N}\epsilon_n(k)\,|\psi_n(k)\rangle\,\langle\psi_n(k)|\right)\mathcal{P}^{-1} = -\mathcal{P}H^{\text{eff}}_{\epsilon}(k)\mathcal{P}^{-1}.
\end{aligned}$$

□

[5] The band index pairing $m \leftrightarrow n$ is completely determined by Eq. (3.6).

Theorem 3. *The operator V_ϵ transforms as*

$$\mathcal{P}V_\epsilon(t,k)\mathcal{P}^{-1} = V_{-\epsilon-2\pi/T}(t,-k)$$

under the particle-hole operator $\mathcal{P}$.

Proof. A straightforward calculation shows that

$$\begin{aligned}
\mathcal{P}V_\epsilon(t,k)\mathcal{P}^{-1} &= \mathcal{P}U(t,k)\mathcal{P}^{-1}\mathcal{P}e^{itH_\epsilon^{\text{eff}}(k)}\mathcal{P}^{-1} = \\
&= U(t,-k)\mathcal{P}\left(\sum_{n=0}^{\infty}\frac{i^n t^n}{n!}H_\epsilon^{\text{eff}}(k)^n\right)\mathcal{P}^{-1} = \\
&= U(t,-k)\sum_{n=0}^{\infty}\frac{(-i)^n t^n}{n!}\left(\mathcal{P}H_\epsilon^{\text{eff}}(k)\mathcal{P}^{-1}\right)^n = \\
&= U(t,-k)\sum_{n=0}^{\infty}\frac{(-i)^n t^n}{n!}\left(-H_{-\epsilon-2\pi/T}^{\text{eff}}(k)\right)^n = \\
&= U(t,-k)e^{itH_{-\epsilon-2\pi/T}^{\text{eff}}(-k)} = V_{-\epsilon-2\pi/T}(t,-k).
\end{aligned}$$

□

Particle-hole symmetry thus provides a link between the gaps at ϵ and $-\epsilon-\frac{2\pi}{T}$.

3.4 Topological invariants

It is time to examine how our topological invariants behave under particle-hole symmetry.

3.4.1 The winding number

As was discussed above, the gap-dependent winding number $w_{\mathcal{C}_t}[V_\epsilon]$ does not have a clear physical interpretation but is still interesting from a mathematical point of view, so it is worthwhile to spend at least a small amount of time examining its properties. First of all, to see why the winding number must be an integer, suppose $\det V_\epsilon(t,0) = e^{i\theta(t)}$ for some real-valued differentiable θ. Then

$$\begin{aligned}
w_{\mathcal{C}_t}[V_\epsilon] &= \frac{1}{2\pi i}\int_{\mathcal{C}_t}\mathrm{d}\log\det V_\epsilon = \frac{1}{2\pi i}\int_0^T\frac{1}{\det V_\epsilon(t,0)}\frac{\partial\det V_\epsilon(t,0)}{\partial t}\,\mathrm{d}t = \\
&= \frac{1}{2\pi i}\int_0^T e^{-i\theta(t)}\left(i\frac{\partial\theta(t)}{\partial t}e^{i\theta(t)}\right)\,\mathrm{d}t = \frac{1}{2\pi}\int_0^T\frac{\partial\theta(t)}{\partial t}\,\mathrm{d}t = \frac{\theta(T)-\theta(0)}{2\pi}.
\end{aligned}$$

Both $\theta(T)$ and $\theta(0)$ must be integer multiples of 2π because $V_\epsilon(T) = V_\epsilon(0) = \mathbb{1}$ has determinant 1, so we end up with an integer value for the winding number. In fact, something even stronger can be said: quasienergies are defined mod $2\pi/T$ so it would make no sense to differentiate between gaps at quasienergies ϵ and $\epsilon+2\pi/T$. As pointed out in ref. [8], this makes the (gap-dependent) winding number of a periodically driven system well-defined only when considered mod N.

Proposition 7. *The winding numbers corresponding to gaps at ϵ and $\epsilon+\frac{2\pi}{T}$ are related by*

$$w_{\mathcal{C}_t}[V_{\epsilon+2\pi/T}] = w_{\mathcal{C}_t}[V_\epsilon] + N,$$

where N is the dimension of the underlying Hilbert space.

Proof. First observe that $H^{\text{eff}}_{\epsilon+2\pi/T}(k) = H^{\text{eff}}_{\epsilon}(k) + \frac{2\pi}{T}\mathbb{1}$, which implies the relation

$$\det\left(V_{\epsilon+2\pi/T}\right) = \det\left(V_\epsilon\right)\det\left(e^{2\pi i\frac{t}{T}\mathbb{1}}\right) = \det\left(V_\epsilon\right)e^{2\pi i N\frac{t}{T}}.$$

The winding number of $V_{\epsilon+2\pi/T}$ can therefore be rewritten on the form

$$\begin{aligned}
w_{\mathcal{C}_t}[V_{\epsilon+2\pi/T}] &= \frac{1}{2\pi i}\int_{\mathcal{C}_t} \mathrm{d}\log\det\left(V_{\epsilon+2\pi/T}\right) = \\
&= \frac{1}{2\pi i}\int_0^T \frac{1}{\det\left(V_{\epsilon+2\pi/T}\right)}\frac{\partial\det\left(V_{\epsilon+2\pi/T}\right)}{\partial t}\,\mathrm{d}t = \\
&= \frac{1}{2\pi i}\int_0^T \frac{1}{\det\left(V_\epsilon\right)e^{2\pi i N\frac{t}{T}}}\left(\frac{\partial\det\left(V_\epsilon\right)}{\partial t}e^{2\pi i N\frac{t}{T}} + \frac{2\pi i N}{T}\det\left(V_\epsilon\right)e^{2\pi i N\frac{t}{T}}\right)\,\mathrm{d}t = \\
&= \frac{1}{2\pi i}\int_0^T \frac{1}{\det\left(V_\epsilon\right)}\frac{\partial\det\left(V_\epsilon\right)}{\partial t}\,\mathrm{d}t + \frac{1}{2\pi i}\int_0^T \frac{2\pi i N}{T}\,\mathrm{d}t = \\
&= \frac{1}{2\pi i}\int_{\mathcal{C}_t}\mathrm{d}\log\det\left(V_\epsilon\right) + N = w_{\mathcal{C}_t}[V_\epsilon] + N,
\end{aligned}$$

which was to be proven. □

Proposition 8. *The gap-dependent winding number in a particle-hole symmetric system satisfies*

$$w_{\mathcal{C}_t}[V_\epsilon] = -w_{\mathcal{C}_t}[V_{-\epsilon-2\pi/T}].$$

Proof. The proof is most clear when $\det V_\epsilon(t,0) = e^{i\theta(t)}$ for some real-valued differentiable θ. Then

$$\det\left(V_{-\epsilon-2\pi/T}\right) = \det\left(\mathcal{P}V_\epsilon\mathcal{P}^{-1}\right) = \det\left(PV_\epsilon^*P^{-1}\right) = \det\left(V_\epsilon^*\right) = \det\left(V_\epsilon\right)^* = e^{-i\theta(t)},$$

so the corresponding winding number simplifies to

$$\begin{aligned}
w_{\mathcal{C}_t}[V_{-\epsilon-2\pi/T}] &= \frac{1}{2\pi i}\int_0^T \frac{1}{\det\left(V_{-\epsilon-2\pi/T}\right)}\frac{\partial\det\left(V_{-\epsilon-2\pi/T}\right)}{\partial t}\mathrm{d}t = \\
&= \frac{1}{2\pi i}\int_0^T e^{i\theta(t)}\left(-i\frac{\partial\theta(t)}{\partial t}e^{-i\theta(t)}\right)\,\mathrm{d}t = -\frac{\theta(T)-\theta(0)}{2\pi} = -w_{\mathcal{C}_t}[V_\epsilon].
\end{aligned}$$

Without the modifying factor $\frac{1}{2\pi i}$, the winding number would be purely imaginary and conjugating the determinant would conjugate the winding number as well, leading to a change in sign; the modifying factor makes the winding number real-valued but the additional minus-sign remains. The general case therefore follows immediately from the equality $\det\left(V_{-\epsilon-2\pi/T}\right) = \det\left(V_\epsilon\right)^*$. □

Together, Propositions 7 & 8 give us the particle-hole symmetry relation

$$w_{\mathcal{C}_t}[V_\epsilon] + w_{\mathcal{C}_t}[V_{-\epsilon}] = N,$$

which is independent of the choice of gap ϵ and need not be taken mod N. A curious special case of this relation is that any system with a gap at $\epsilon = 0$ has winding number $w_{\mathcal{C}_t}[V_0] = N/2$, which is only possible if the Hilbert space dimension N is even. This result may seem surprising but it actually strengthens a similar result that could have been obtained earlier: In any particle-hole symmetric system of odd dimension, there is an odd number of (not necessarily distinct) bands λ_n so at least one of them must be its own particle-hole symmetric partner at $k = 0$, in the sense of setting $n = m$ in Eq. (3.6). The corresponding eigenvalue $\lambda_n(0) = \lambda_n(0)^*$ is then real-valued and closes the gap at either $\epsilon = 0$ or $\epsilon = \pi/T$, so an odd-dimensional system cannot be gapped at both of these quasienergies. What the stronger result $w_{\mathcal{C}_t}[V_0] = N/2$ says is that an odd-dimensional system cannot be gapped at $\epsilon = 0$.

3.4.2 The degree

Recall that the degree is a $\pi_3(U(N)) \simeq \mathbb{Z}$ topological invariant given by the integral

$$\deg(V) = \frac{1}{8\pi^2} \int_{\mathbb{T}^3} \operatorname{tr}\left(V^\dagger \partial_t V \left[V^\dagger \partial_{k_x} V, V^\dagger \partial_{k_y} V\right]\right) \mathrm{d}k_x \wedge \mathrm{d}k_y \wedge \mathrm{d}t \tag{3.7}$$

for maps $V : \mathbb{T}^3 \to U(N)$. As was discussed earlier, the gap-dependent degree is our most important topological invariant due to its interpretation as the number of chiral edge states traversing the chosen quasienergy gap: $\deg V_\epsilon = n_{\mathrm{edge}}(\epsilon)$. Establishing a relation between the degrees of V_ϵ and $V_{-\epsilon-2\pi/T}$ would therefore enable us to draw concrete conclusions about the underlying physics. It is difficult to see how the expression (3.7) behaves under transformations of V, however, so we rewrite it on a simpler form as the integral

$$\deg(V) = \frac{1}{24\pi^2} \int_{\mathbb{T}^3} V^*\chi, \tag{3.8}$$

of the differential form[6] $V^*\chi = \operatorname{tr}(\Theta \wedge \Theta \wedge \Theta)$, where $\Theta = V^{-1}\mathrm{d}V$.

Lemma 7. *The integrals* (3.7) *and* (3.8) *coincide.*

Proof. We begin by examining the differential 3-form $V^*\chi$. By definition,

$$\Theta = V^{-1}\mathrm{d}V = V^\dagger \mathrm{d}V = V^\dagger \left(\frac{\partial V}{\partial k_x}\mathrm{d}k_x + \frac{\partial V}{\partial k_y}\mathrm{d}k_y + \frac{\partial V}{\partial t}\mathrm{d}t\right),$$

and a tedious but straightfoward calculation shows that

$$\Theta \wedge \Theta = \left[V^\dagger V'_{k_x}, V^\dagger V'_{k_y}\right]\mathrm{d}k_x \wedge \mathrm{d}k_y + \left[V^\dagger V'_{k_x}, V^\dagger V'_t\right]\mathrm{d}k_x \wedge \mathrm{d}t + \left[V^\dagger V'_{k_y}, V^\dagger V'_t\right]\mathrm{d}k_y \wedge \mathrm{d}t.$$

An equally tedious but equally straightforward calculation then yields the expression

$$\Theta\wedge\Theta\wedge\Theta = \left(V^\dagger V'_t\left[V^\dagger V'_{k_x}, V^\dagger V'_{k_y}\right] + V^\dagger V'_{k_x}\left[V^\dagger V'_{k_y}, V^\dagger V'_t\right] + V^\dagger V'_{k_y}\left[V^\dagger V'_t, V^\dagger V'_{k_x}\right]\right)\mathrm{d}k_x \wedge \mathrm{d}k_y \wedge \mathrm{d}t,$$

which we can rewrite as

$$\left(V^\dagger \partial_t V\left[V^\dagger \partial_{k_x} V, V^\dagger \partial_{k_y} V\right] + V^\dagger \partial_{k_x} V\left[V^\dagger \partial_{k_y} V, V^\dagger \partial_t V\right] + V^\dagger \partial_{k_y} V\left[V^\dagger \partial_t V, V^\dagger \partial_{k_x} V\right]\right)\mathrm{d}k_x \wedge \mathrm{d}k_y \wedge \mathrm{d}t.$$

This expression is on the form $A\big[B,C\big] + B\big[C,A\big] + C\big[A,B\big]$ for

$$A := V^\dagger \partial_t V, \qquad B := V^\dagger \partial_{k_x} V, \qquad C := V^\dagger \partial_{k_y} V,$$

meaning that the three terms are cyclic permutations of each other. As the trace is a linear function which is invariant under cyclic permutations, it follows that

$$\operatorname{tr}\left(A\big[B,C\big] + B\big[C,A\big] + C\big[A,B\big]\right) = 3\operatorname{tr}\left(A\big[B,C\big]\right),$$

proving the relation

$$V^*\chi = \operatorname{tr}(\Theta \wedge \Theta \wedge \Theta) = 3\operatorname{tr}\left(V^\dagger \partial_t V\left[V^\dagger \partial_{k_x} V, V^\dagger \partial_{k_y} V\right]\right)\mathrm{d}k_x \wedge \mathrm{d}k_y \wedge \mathrm{d}t.$$

Consequently,

$$\frac{1}{24\pi^2}\int_{\mathbb{T}^3} V^*\chi = \frac{1}{8\pi^2}\int_{\mathbb{T}^3} \operatorname{tr}\left(V^\dagger \partial_t V\left[V^\dagger \partial_{k_x} V, V^\dagger \partial k_y V\right]\right)\mathrm{d}k_x \wedge \mathrm{d}k_y \wedge \mathrm{d}t.$$

□

[6] The notation $V^*\chi$ comes from ref. [8] and emphasizes that $V^*\chi$ is the pullback along V of a 3-form χ on $U(N)$.

Let us keep the ball rolling by presenting a number of additional, equally important results.

Lemma 8. *The 3-form $V^*\chi$ is a real 3-form.*

Proof. The equality

$$0 = \partial_t \mathbb{1} = \partial_t V^\dagger V = \frac{\partial V^\dagger}{\partial t} V + V^\dagger \frac{\partial V}{\partial t}$$

implies that $A = V^\dagger \partial_t V$ is anti-Hermitian:

$$V^\dagger \frac{\partial V}{\partial t} = -\frac{\partial V^\dagger}{\partial t} V = -\left(\frac{\partial V}{\partial t}\right)^\dagger V = -\left(V^\dagger \frac{\partial V}{\partial t}\right)^\dagger,$$

and the same holds for $B = V^\dagger \partial_{k_x} V$ and $C = V^\dagger \partial_{k_y} V$. The commutator of two anti-Hermitian matrices is easily seen to be anti-Hermitian, so the trace

$$\operatorname{tr}\big(A[B,C]\big) = \operatorname{tr}\big([B,C]A\big) = \operatorname{tr}\Big(\big(A[B,C]\big)^\dagger\Big) = \operatorname{tr}\big(A[B,C]\big)^*$$

is real-valued and we conclude that

$$V^*\chi = 3 \operatorname{tr}\big(A[B,C]\big)\, \mathrm{d}k_x \wedge \mathrm{d}k_y \wedge \mathrm{d}t$$

is a real 3-form. □

Lemma 9. *The degree satisfies*

$$\deg V_1 V_2 = \deg V_1 + \deg V_2,$$

for any pair of maps V_1, V_2.

Proof. See [8] for details. □

Corollary 3.

(a) *The degree is invariant under particle-hole transformations:*

$$\deg \mathcal{P} V \mathcal{P}^{-1} = \deg V,$$

for all maps $V : \mathbb{T}^3 \to U(N)$

(b) *The degree satisfies*

$$\deg V_{\epsilon + 2\pi/T} = \deg V_\epsilon$$

for any quasienergy ϵ.

Proof.

(a) Let P be the unitary part of the particle-hole operator $\mathcal{P} = P\mathcal{K}$. Then

$$\deg P^{-1} = \deg P P^{-1} - \deg P = \underbrace{\deg \mathbb{1}}_{=0} - \deg P = -\deg P,$$

so the degree simplifies to

$$\deg \mathcal{P} V \mathcal{P}^{-1} = \deg P V^* P^{-1} = \deg P + \deg V^* - \deg P = \deg V^* = \deg V,$$

where the last equality follows from the reality of the 3-form $V^*\chi$.

(b) The maps $V_{\epsilon+2\pi/T}$ and V_ϵ are clearly related by

$$V_{\epsilon+2\pi/T}(k,t) = V_\epsilon(k,t)e^{\frac{2\pi i t}{T}\mathbb{1}} = V_\epsilon(k,t)e^{\frac{2\pi i t}{T}}\mathbb{1},$$

which implies that

$$\deg V_{\epsilon+2\pi/T} = \deg V_\epsilon + \deg e^{2\pi i t/T}\mathbb{1},$$

and it is not difficult to see that the second term vanishes.

□

After this series of lemmas and corollaries, we arrive at our main result.

Theorem 4. *The degree of a particle-hole symmetric Floquet topological insulator satisfies*

$$\deg V_\epsilon = \deg V_{-\epsilon}$$

for any gap ϵ. The numbers of chiral edge states at quasienergies $\pm\epsilon$ are therefore equal.

We find this succinct result beautiful as it reflects the mirror-symmetry in the Floquet spectrum. It is also natural in hindsight, since any electronic state at quasienergy ϵ should be accompanied by a hole state at quasienergy $-\epsilon$ and the system is not allowed to change when we interchange the roles of electrons and holes. In other words, our result captures the defining characteristics of particle-hole symmetry and helps validate the conceptual accuracy of the underlying theory.

Before ending this chapter, let us briefly discuss Chern numbers. Suppose that ϵ and ϵ' represent two distinct gaps such that $\epsilon < \epsilon'$ and observe that the product $V_\epsilon^{-1}V_{\epsilon'}$ has the simple form

$$V_\epsilon^{-1}V_{\epsilon'} = \left(e^{-itH_\epsilon^{\text{eff}}(k)}U(t,k)^{-1}\right)\left(U(t,k)e^{itH_{\epsilon'}^{\text{eff}}(k)}\right) = \exp\left[it\Big(H_{\epsilon'}^{\text{eff}}(k) - H_\epsilon^{\text{eff}}(k)\Big)\right],$$

where

$$H_{\epsilon'}^{\text{eff}}(k) - H_\epsilon^{\text{eff}}(k) = \sum_n \Big[\ln_{\epsilon'}\big(\lambda_n(k)\big) - \ln_\epsilon\big(\lambda_n(k)\big)\Big]P_n(k).$$

Assuming that $|\epsilon' - \epsilon| < 2\pi/T$, the coefficient functions $\ln_{\epsilon'}\big(\lambda_n(k)\big) - \ln_\epsilon\big(\lambda_n(k)\big)$ vanish identically for all bands outside the interval (ϵ, ϵ') whilst the (intermediate) bands located inside the interval experience a $2\pi/T$ phase difference between the two logarithms, leading to the simplified expression

$$H_{\epsilon'}^{\text{eff}}(k) - H_\epsilon^{\text{eff}}(k) = \frac{2\pi}{T}\sum_{\substack{\text{intermediate}\\ \text{bands}}} P_n(k).$$

That is, the product $V_\epsilon^{-1}V_{\epsilon'}$ only depends on those bands which lie inside the interval (ϵ, ϵ'). With this in mind, we are not surprised to learn that the change in the number of chiral edge states,

$$\mathcal{C}_{\epsilon,\epsilon'} = n_{\text{edge}}(\epsilon') - n_{\text{edge}}(\epsilon) = \deg V_{\epsilon'} - \deg V_\epsilon = \deg V_\epsilon^{-1}V_{\epsilon'},$$

equals the total Chern number of the intermediate bands [26]. Theorem 4 therefore enables us to make some observations about the Chern numbers of a particle-hole symmetric system.

Corollary 4. *The total Chern number of all bands in the interval $(-\epsilon, \epsilon)$ vanishes, for any gap ϵ.*

Proof. Theorem 4 immediately implies that

$$\mathcal{C}_{-\epsilon,\epsilon} = \deg V_\epsilon - \deg V_{-\epsilon} = 0.$$

□

The above results do not provide any tools with which to study Chern numbers of individual bands, we can only calculate the total Chern number of all bands in an interval (ϵ, ϵ') between two gaps ϵ, ϵ'. It is still possible to draw interesting conclusions, however, by restricting attention to *arcs* $A_{\epsilon,\epsilon'}$ which we define as the union of all bands located between two *adjacent* gaps ϵ, ϵ'. For example, the Floquet spectrum shown in Figure 3.6 consists of three arcs, each with a corresponding Chern number, even though the total number of individual bands may be much larger. Observe that if $A_{\epsilon,\epsilon'}$ is an arc, then so is $A_{-\epsilon',-\epsilon}$ due to the mirror symmetry of the Floquet spectrum and we call these two arcs *complementary*. If ϵ and $-\epsilon$ are adjacent and distinct gaps, which can only happen in a system which is gapless at either $\epsilon = 0$ or $\epsilon = \pi/T$, then the arc $A_{\epsilon,-\epsilon}$ is self-complementary.

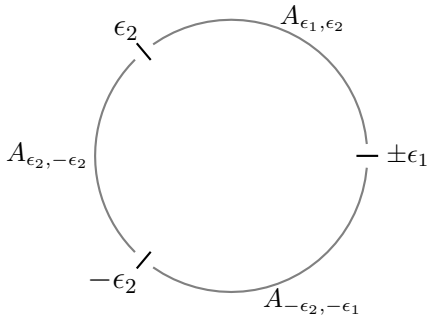

Figure 3.6: Chern numbers $\mathcal{C}_{\epsilon,\epsilon'}$ can be calculated for each *arc* $A_{\epsilon,\epsilon'}$, defined as the union of all quasienergy bands located between two adjacent gaps with respective midpoint ϵ, ϵ'. Each arc $A_{\epsilon,\epsilon'}$ is complementary to another arc $A_{-\epsilon',-\epsilon}$ and the two coincide if $\epsilon' = -\epsilon$.

Corollary 5. *Complementary arcs have opposite Chern numbers:*

$$\mathcal{C}_{-\epsilon',-\epsilon} = -\mathcal{C}_{\epsilon,\epsilon'}.$$

In particular, self-complementary arcs have vanishing Chern numbers.

Proof. Let $\epsilon_1, \ldots, \epsilon_M$ denote the midpoint of each gap on the upper half of the unit circle, so that

$$0 \leq \epsilon_1 < \epsilon_2 < \cdots < \epsilon_M \leq \frac{\pi}{T}.$$

The corresponding midpoints of gaps on the lower half of the unit circle are simply $-\epsilon_1, \ldots, -\epsilon_M$. A system which is gapless at $\epsilon = 0$ has a single, self-complementary arc $A_{-\epsilon_1,\epsilon_1}$ in the interval $(-\epsilon_1, \epsilon_1)$ and its Chern number $\mathcal{C}_{-\epsilon_1,\epsilon_1}$ vanishes per Corollary 4. If the system is gapped at $\epsilon = 0$, on the other hand, then $\epsilon_1 = 0$ and the interval $(-\epsilon_1, \epsilon_1)$ is empty. The larger interval $(-\epsilon_2, \epsilon_2)$ contains two additional arcs $A_{\epsilon_1,\epsilon_2}$ and $A_{-\epsilon_2,-\epsilon_1}$ which are complementary to each other, and it is easy to see that

$$\mathcal{C}_{-\epsilon_2,-\epsilon_1} + \underbrace{\mathcal{C}_{-\epsilon_1,\epsilon_1}}_{0} + \mathcal{C}_{\epsilon_1,\epsilon_2} = \mathcal{C}_{-\epsilon_2,\epsilon_2} = 0,$$

which proves that $\mathcal{C}_{-\epsilon_2,-\epsilon_1} = -\mathcal{C}_{\epsilon_1,\epsilon_2}$. The result now follows by repeating the same argument iteratively for each successively larger interval $(-\epsilon_3, \epsilon_3), \ldots, (-\epsilon_M, \epsilon_M)$. □

3.5 Discussion

Our focus in this final chapter has been on periodically driven systems with particle-hole symmetry. We proved that any such system has a mirror-symmetric Floquet spectrum consisting of $N = \dim \mathcal{H}$ quasienergy bands and a finite number of quasienergy gaps. Inside each gap, which we denote by ϵ, there may exist a number of chiral edge states and our main result says that these numbers reflect the mirror-symmetry in the spectrum:

$$n_{\text{edge}}(\epsilon) = n_{\text{edge}}(-\epsilon).$$

In other words, any chiral edge state inside a quasienergy gap ϵ is accompanied by another chiral edge state inside the quasienergy gap $-\epsilon$, and we argued that this is a natural result given the defining characteristics of particle-hole symmetry.

The gap-dependent winding number $w_{\mathcal{C}_t}[V_\epsilon]$ was proven to be a $\mathbb{Z}_N$-valued quantity that in some cases provides information about the underlying Hilbert space. For example, we showed that an odd-dimensional particle-hole symmetric system cannot be gapped at quasienergy $\epsilon = 0$. The question whether the winding number has a physical interpretation remains unanswered but we do not believe such an interpretation exists. It should be possible, for example, to add "physically irrelevant" quasienergy bands with vanishing Chern numbers, in a way that preserves particle-hole symmetry and does not create any new gap. However, the process of adding additional bands increases the Hilbert space dimension and thereby changes the winding numbers. We think that quantities which depend on the Hilbert space dimension are unlikely to carry physical information.

One way to extend our work in this thesis would be to analyse what happens when "irrelevant" bands are either added or removed. It is conceivable for such an analysis to reveal surprising properties of periodically driven systems, as the $2\pi/T$ periodicity of the quasienergy spectrum blurs the lines between low and high quasienergies; between occupied and unoccupied bands. Rigorous analysis of these questions cannot be conducted within the context of homotopy theory, but require more sophisticated techniques which are able to compare systems of different dimensions.

References

[1] Alicea, J., Oreg, Y., Refael, G., Von Oppen, F., & Fisher, M. P. (2011). Non-Abelian statistics and topological quantum information processing in 1D wire networks. Nature Physics, 7(5), 412.

[2] Altland, A., & Zirnbauer, M. R. (1997). Nonstandard symmetry classes in mesoscopic normal-superconducting hybrid structures. Physical Review B, 55(2), 1142.

[3] Bernevig, B. A., & Hughes, T. L. (2013). Topological insulators and topological superconductors. Princeton university press.

[4] Berry, M. V. (1984). Quantal phase factors accompanying adiabatic changes. Proceedings of the Royal Society of London. A. Mathematical and Physical Sciences, 392(1802), 45-57.

[5] Bott, R., and R. Seeley. "Some remarks on the paper of Callias." Communications in Mathematical Physics 62.3 (1978) : 235-2 45.

[6] Bradlyn, B., Elcoro, L., Cano, J., Vergniory, M. G., Wang, Z., Felser, C., ... & Bernevig, B. A. (2017). Topological quantum chemistry. Nature, 547(7663), 298.

[7] Caponigro, M. (2008). Interpretations of Quantum Mechanics: a critical survey. arXiv preprint arXiv:0811.3877.

[8] Carpentier, D., Delplace, P., Fruchart, M., & Gawędzki, K. (2015). Topological index for periodically driven time-reversal invariant 2D systems. Physical review letters, 114(10), 106806.

[9] Chiu, C. K., Teo, J. C., Schnyder, A. P., & Ryu, S. (2016). Classification of topological quantum matter with symmetries. Reviews of Modern Physics, 88(3), 035005.

[10] Debnath, L., & Mikusiński, P. (2005). Hilbert spaces with applications. Academic press.

[11] Dirac, P. A. M. (1939, July). A new notation for quantum mechanics. In Mathematical Proceedings of the Cambridge Philosophical Society (Vol. 35, No. 3, pp. 416-418). Cambridge University Press.

[12] Dirac, P. A. M. (1981). The principles of quantum mechanics (No. 27). Oxford university press.

[13] Haldane, F. D. M. (1988). Model for a quantum Hall effect without Landau levels: Condensed-matter realization of the" parity anomaly". Physical Review Letters, 61(18), 2015.

[14] Joachain, C. J. (1975). Quantum collision theory.

[15] Kane, C. L., & Mele, E. J. (2005). Quantum spin Hall effect in graphene. Physical review letters, 95(22), 226801.

[16] Kato, T. (2013). Perturbation theory for linear operators (Vol. 132). Springer Science & Business Media.

[17] Kitagawa, T., Berg, E., Rudner, M., & Demler, E. (2010). Topological characterization of periodically driven quantum systems. Physical Review B, 82(23), 235114.

[18] Kittel, C., McEuen, P., & McEuen, P. (1996). Introduction to solid state physics. Vol. 8. New York: Wiley.

[19] Klitzing, K. V., Dorda, G., & Pepper, M. (1980). New method for high-accuracy deter mination of the fine-structure constant based on quantized Hall resistance. Physical Review Letters, 45(6), 494.

[20] Lee J.M. (2013) Lie Groups. In: Introduction to Smooth Manifolds. Graduate Texts in Mathematics, vol 218. Springer, New York, NY

[21] Lindner, N. H., Refael, G., & Galitski, V. (2011). Floquet topological insulator in semiconductor quantum wells. Nature Physics, 7(6), 490.

[22] Peng, Y. G., Qin, C. Z., Zhao, D. G., Shen, Y. X., Xu, X. Y., Bao, M., ... & Zhu, X. F. (2016). Experimental d emonstration of anomalous Floquet topological insulator for sound. Nature communications, 7, 13368.

[23] Rechtsman, M. C., Zeuner, J. M., Plotnik, Y., Lumer, Y., Podolsky, D., Dreisow, F., ... & Szameit, A.x (2013). Photonic Floquet topological insulators. Nature, 496(7444), 196.

[24] Mong, R. S., & Shivamoggi, V. (2011). Edge states and the bulk-boundary correspondence in Dirac Hamiltonians. Physical Review B, 83(12), 125109.

[25] Roy, R., & Harper, F. (2017). Periodic table for floquet topological insulators. Physical Review B, 96(15), 155118.

[26] Rudner, M. S., Lindner, N. H., Berg, E., & Levin, M. (2013). Anomalous edge states and the bulk-edge correspondence for periodically driven two-dimensional systems. Physical Review X, 3(3), 031005.

[27] Sakurai, J. J., & Napolitano, J. J. (2014). Modern quantum mechanics. Pearson Higher Ed.

[28] Sato, M., & Ando, Y. (2017). Topological superconductors: a review. Reports on Progress in Physics, 80(7), 076501.

[29] Schlosshauer, M. (2005). Decoherence, the measurement problem, and interpretations of quantum mechanics. Reviews of Modern physics, 76(4), 1267.

[30] Schwichtenberg, J. (2015). Physics from Symmetry. Heidelberg: Springer.

[31] Shankar, R. (2012). Principles of quantum mechanics. Springer Science & Business Media.

[32] Shen, S. Q. (2012). Topological insulators (Vol. 174). New York: Springer.

[33] Stanescu, T. D. (2016). Introduction to Topological Quantum Matter & Quantum Computation. CRC Press.

[34] Thouless, D. J., Kohmoto, M., Nightingale, M. P., & den Nijs, M. (1982). Quantized Hall conductance in a two-dimensional periodic potential. Physical Review Letters, 49(6), 405.

[35] Wang, Y. H., Steinberg, H., Jarillo-Herrero, P., & Gedik, N. (2013). Observation of Floquet-Bloch states on the surface of a topological insulator. Science, 342(6157), 453-457.

[36] Zhang, Y., Tan, Y. W., Stormer, H. L., & Kim, P. (2005). Experimental observation of the quantum Hall effect and Berry's phase in graphene. nature, 438(7065), 201.

[37] http://www.reed.edu/physics/faculty/wheeler/documents/QuantumMechanics/MiscellaneousEssays/Ehrenfest'sTheorem.pdf

[38] https://commons.wikimedia.org/wiki/File:Band_filling_diagram.svg